RESEARCH ARTICLE | *Control of Movement*

The serotonin reuptake blocker citalopram destabilizes fictive locomotor activity in salamander axial circuits through 5-HT$_{1A}$ receptors

Aurélie Flaive,[1] Jean-Marie Cabelguen,[2] and ![ORCID] Dimitri Ryczko[1,3,4,5]

[1]*Département de Pharmacologie-Physiologie, Faculté de médecine et des sciences de la santé, Université de Sherbrooke, Sherbrooke, Quebec, Canada;* [2]*Neurocentre Magendie, INSERM U 862, Université de Bordeaux, Bordeaux Cedex, France;* [3]*Centre de recherche du Centre Hospitalier Universitaire de Sherbrooke, Sherbrooke, Quebec, Canada;* [4]*Institut de Pharmacologie de Sherbrooke, Sherbrooke, Quebec, Canada; and* [5]*Centre des neurosciences de Sherbrooke, Sherbrooke, Quebec, Canada*

Flaive A, Cabelguen JM, Ryczko D. The serotonin reuptake blocker citalopram destabilizes fictive locomotor activity in salamander axial circuits through 5-HT$_{1A}$ receptors. *J Neurophysiol* 123: 2326–2342, 2020. First published May 13, 2020; doi:10.1152/jn.00179.2020.—Serotoninergic (5-HT) neurons are powerful modulators of spinal locomotor circuits. Most studies on 5-HT modulation focused on the effect of exogenous 5-HT and these studies provided key information about the cellular mechanisms involved. Less is known about the effects of increased release of endogenous 5-HT with selective serotonin reuptake inhibitors. In mammals, such molecules were shown to destabilize the fictive locomotor output of spinal limb networks through 5-HT$_{1A}$ receptors. However, in tetrapods little is known about the effects of increased 5-HT release on the locomotor output of axial networks, which are coordinated with limb circuits during locomotion from basal vertebrates to mammals. Here, we examined the effect of citalopram on fictive locomotion generated in axial segments of isolated spinal cords in salamanders, a tetrapod where raphe 5-HT reticulospinal neurons and intraspinal 5-HT neurons are present as in other vertebrates. Using electrophysiological recordings of ventral roots, we show that fictive locomotion generated by bath-applied glutamatergic agonists is destabilized by citalopram. Citalopram-induced destabilization was prevented by a 5-HT$_{1A}$ receptor antagonist, whereas a 5-HT$_{1A}$ receptor agonist destabilized fictive locomotion. Using immunofluorescence experiments, we found 5-HT-positive fibers and varicosities in proximity with motoneurons and glutamatergic interneurons that are likely involved in rhythmogenesis. Our results show that increasing 5-HT release has a deleterious effect on axial locomotor activity through 5-HT$_{1A}$ receptors. This is consistent with studies in limb networks of turtle and mouse, suggesting that this part of the complex 5-HT modulation of spinal locomotor circuits is common to limb and axial networks in limbed vertebrates.

NEW & NOTEWORTHY Little is known about the modulation exerted by endogenous serotonin on axial locomotor circuits in tetrapods. Using axial ventral root recordings in salamanders, we found that a serotonin reuptake blocker destabilized fictive locomotor activity through 5-HT$_{1A}$ receptors. Our anatomical results suggest that serotonin is released on motoneurons and glutamatergic interneurons possibly involved in rhythmogenesis. Our study suggests that common serotoninergic mechanisms modulate axial motor circuits in amphibians and limb motor circuits in reptiles and mammals.

Correspondence: D. Ryczko (dimitri.ryczko@usherbrooke.ca).

INTRODUCTION

The salamander locomotor circuitry shares many similarities with that of other vertebrates. In the brainstem, stimulation of the mesencephalic locomotor region evokes slow stepping movements at low stimulation intensity, and faster swimming movements at higher intensities (Cabelguen et al. 2003). This region does so by controlling the level of activation of reticulospinal neurons, which relay the locomotor command to the spinal cord (Chevallier et al. 2004; Ryczko et al. 2016a). The salamander spinal cord contains an axial central pattern generator organized as a double chain of "unit burst generators" (Grillner 1981) that coordinate their activity to generate the pattern of axial movements in the trunk (Delvolvé et al. 1999; Ryczko et al. 2010, 2015) and tail (Charrier and Cabelguen 2013) as in lamprey (Cangiano and Grillner 2003, 2005). The salamander spinal cord also contains central pattern generators for limb movements composed of "unit burst generators" (Cheng et al. 1998, 2002; Jovanović et al. 1999; Lavrov and Cheng 2008), as described in the mouse spinal cord (Hägglund et al. 2013). Salamander motoneurons integrate premotor signals and send their output to the muscles (Chevallier et al. 2006, 2008). Electrophysiological studies based on ventral root (VR) recordings showed that, within the salamander axial network, glutamatergic synapses are essential to generate rhythmic bursts of activity and inhibitory glycinergic neurons coordinate the alternation of left and right sides (Ryczko et al. 2010). This phenomenon and also the role of neuronal intrinsic properties in the modulation of rhythm speed and stability (Ryczko et al. 2010) were modeled using a network of Hodgkin-Huxley neurons (Bicanski et al. 2013).

Serotoninergic (5-HT) neurons are present in the salamander brain (Branchereau et al. 2000; Corio et al. 1992; Dubé and Parent 1982; Fasolo et al. 1986; Haraguchi et al. 2012; Harris 1983; Lowry et al. 1996, 2001, 2009; Norris et al. 1992; O'Brien et al. 2004). In the spinal cord, an abundant 5-HT innervation was described (Branchereau et al. 2000; Jovanović et al. 1996), as in other vertebrates (e.g., lamprey:

Harris-Warrick et al. 1985; mouse: Dunbar et al. 2010). The brain provides a large part of the spinal 5-HT innervation, as shown by the major loss of spinal 5-HT fibers following spinal cord transection at the level of the second spinal segment (Branchereau et al. 2000). The salamander raphe nucleus in the caudal brainstem contains 5-HT neurons (Clairambault et al. 1994; Hubbard et al. 2010) among which some project to the spinal cord (Chevallier et al. 2004). In addition, 5-HT neurons are present in the spinal cord of salamanders (Branchereau et al. 2000; Jovanović et al. 1996; Sims 1977) as in other vertebrates (e.g., lamprey: Harris-Warrick et al. 1985; mouse: Ballion et al. 2002; turtle: Fabbiani et al. 2018).

The application of exogenous 5-HT was reported to slow down the fictive locomotor rhythm generated by the axial network (Branchereau et al. 2000) and limb networks (Jovanović et al. 1996) evoked by bath-applied glutamatergic agonists. However, less is known about the effects of increased release of endogenous 5-HT with 5-HT reuptake inhibitors (SSRI), which block the serotonin transporter (SERT). Intriguingly, such molecules destabilize fictive locomotion (lamprey: Christenson et al. 1989; mouse: Dunbar et al. 2010) and fictive scratching (turtle: Perrier et al. 2018) and such effects were linked to the activation of 5-HT$_{1A}$ receptors (Cotel et al. 2013; Dunbar et al. 2010). Such deleterious effects of SSRIs were not systematically examined when applying exogenous 5-HT in reduced preparations. This apparent contrast between the effects of exogenous and endogenous 5-HT was proposed to be related, among other reasons, to the level of 5-HT release that can recruit either synaptic or extrasynaptic receptors (for review, see Perrier and Cotel 2015). In salamander axial circuits, the effects of increasing the endogenous release of 5-HT on rhythm stability were not previously investigated. Moreover, the receptors involved in the 5-HT modulation of locomotor activity and the possible targets of the spinal 5-HT fibers are largely unknown.

Here, we examined whether increase of endogenous 5-HT release using the SSRI citalopram modulates axial fictive locomotor activity evoked by bath-applied glutamatergic agonists [N-methyl-D-aspartate (NMDA) and D-serine] in the isolated spinal cord of salamanders. We investigated the role of 5-HT$_{1A}$ receptors that were reported to destabilize locomotor activity in mammals (Dunbar et al. 2010) as well as scratching activity (Perrier et al. 2018) by acting at the motoneuronal level (Cotel et al. 2013). The presence of 5-HT$_{1A}$ receptors in salamanders was previously described using gene sequencing (Reyes-Ruiz et al. 2013) and patch-clamp recordings in taste buds (Delay et al. 1997). Using immunofluorescence experiments, we examined whether 5-HT fibers were present around motoneurons and ventral glutamatergic neurons, which play a key role in rhythm generation in salamanders (Bicanski et al. 2013; Ryczko et al. 2010) as in other vertebrates (for review, see Kiehn 2016).

MATERIALS AND METHODS

Ethics statement. The procedures conformed to the guidelines of the Canadian Council on Animal Care and were approved by the animal care and use committees of the Université de Sherbrooke (Sherbrooke, QC, Canada), Université de Bordeaux (France), and INSERM Ethics Committee (permit number A50120148). Care was taken to minimize the number of animals used and their suffering.

Animals. A total of 25 salamanders was used for the present study. Considering the difficulty to have access to salamanders because of the emerging fungal pathogen *Batrachochytrium salamandrivorans* (for review, see Gray et al. 2015), we had to use two different species for physiology and anatomy experiments in the present study. For electrophysiology experiments, 21 Iberian newts (*Pleurodeles waltl*) with snout–vent length ranging from 5 to 9 cm were purchased from Blades Biological Ltd. (UK) and fed twice per week with Chironomidae larvae and veal heart. For anatomical experiments, we used 4 Mexican axolotls (*Ambystoma mexicanum*) purchased from the Ambystoma Genetic Stock Center (University of Kentucky) with snout–vent length ranging from 8 to 12 cm. The animals were kept in aquariums at 17–19°C and fed twice per week with fish pellets. The sex of the animals was not taken into account.

Surgical procedures. The animals were anesthetized with tricaine methanesulfonate (MS-222, 200 mg/mL, Sigma) and then transferred into a cold oxygenated Ringer's solution (in mM:130 NaCl, 2.1 KCl, 2.6 CaCl$_2$, 1.8 MgCl$_2$, 4 HEPES, 5 glucose, and 1 NaHCO$_3$, pH = 7.4). The skin and the muscles were removed. A dorsal laminectomy was performed to provide access to the first 20 segments of the spinal cord. The spinal cord was isolated from the brain by a transverse section at the level of the obex. Following this step, the preparations were prepared for either anatomy or physiology experiments. For anatomy experiments, we surgically isolated the axial segments innervating the trunk muscles (segments 9 to 11 in $n = 3$ animals) or tail muscles (segment 20 in $n = 1$ animal) using transverse sections applied between VRs (Charrier and Cabelguen 2013; Delvolvé et al. 1999; Ryczko et al. 2010, 2015). For electrophysiology experiments, VRs innervating the trunk muscles (VR6 to VR13) were dissected from surrounding tissues and cut transversally to provide easy access to the suction electrodes. The whole spinal cord preparation was then transferred to a Sylgard recording chamber, pinned down, dorsal side up, and superfused (5 mL/min) with a cold (7°C) oxygenated Ringer's solution containing the neuromuscular blocking agent α-bungarotoxin (2 μM, Sigma). After 12 h of recovery, the temperature of the Ringer's solution was raised to 17°C before recordings began.

Electrophysiology. Extracellular recordings of VR activity were performed with glass suction electrodes as previously described (Charrier and Cabelguen 2013; Delvolvé et al. 1999; Ryczko et al. 2010, 2015). Briefly, the neurograms were amplified ($\times$10,000), band-pass filtered (10 Hz–1 kHz) and digitized (4.8 kHz) with a Micro-1401mk II system bundled with Spike2 (Cambridge Electronic Design, UK). Rhythmic activities were evoked by bath-applying a Ringer's solution containing N-methyl-D-aspartate (NMDA, 20 μM) and D-serine (10 μM) (Sigma) (Charrier and Cabelguen 2013; Delvolvé et al. 1999; Ryczko et al. 2010, 2015). The recordings began when stable patterns of activities had emerged after 1 h of bath application of NMDA and D-serine. Bouts of motor activity recorded from VRs were rectified and filtered with a time constant of 50 ms using Spike2 scripts (Ryczko et al. 2010, 2015). Wavelet transformations and analyses were done on the rectified and filtered signals using Spinalcore software run in MATLAB (MathWorks) as previously done in rats (Beliez et al. 2015; Mor and Lev-Tov 2007) mice (Hägglund et al. 2013; Sharples and Whelan 2017) and salamanders (Ryczko et al. 2015). The cross-power was obtained with the cross-wavelet transform algorithm (XWT; see Mor and Lev-Tov 2007) which reveals the shared rhythm frequency bands over time but does not provide the significance of the correlation between the two VR signals. Such significance was obtained by determining the rhythm coherence between the two VR signals with the wavelet transform coherence algorithm (CWT; see Mor and Lev-Tov 2007), which calculates the coherence as a normalized cross-spectral density function on a scale from 0 to 1 and tests coherence significance over time for each given rhythm frequency using Monte Carlo simulations against white noise (Mor and Lev-Tov 2007; Wang et al. 2004). The coherent cross-power (CXWT; see Mor and Lev-Tov 2007) is a

graphical representation that combines the results of the CWT and XWT into a single density plot of the cross-power from which the nonsignificantly coherent cross-power (computed using CWT) was removed. In CXWT plots, color coding was used to illustrate the cross-power between two VR signals in time-frequency domains. The time-frequency domains with high cross-power that were in the close neighborhood of the motor rhythm frequency were delineated graphically and used for statistical analysis of the rhythm coherence and phase lag between the two VR signals. The raw phase relationship between signals is illustrated as a vector on a circular plot. The phase lag per segment was obtained by converting the phase in percentage and dividing it by the intervening number of segments (Ryczko et al. 2015).

Drugs. Drugs were purchased from Sigma and diluted to their final concentration in Ringer's solution and bath-applied over the spinal cord preparation. NMDA (20 μM) and D-serine (10 μM) were used to elicit fictive locomotion (Charrier and Cabelguen 2013; Delvolvé et al. 1999; Ryczko et al. 2010, 2015). We tested the effects of 5-HT drugs after 30 min of bath application. To increase the release of endogenous 5-HT we used the SSRI citalopram at 0.1, 1, 2.5, and 5 μM (Christenson et al. 1989; Dunbar et al. 2010). To activate 5-HT$_{1A}$ receptors we used the 5-HT$_{1A}$ agonist 8-OH-DPAT (0.1 μM, 1 μM) (Wang et al. 2011). To block 5-HT$_{1A}$ receptors we used the 5-HT$_{1A}$ antagonist WAY-100635 (1 μM) (Dunbar et al. 2010).

Immunofluorescence experiments. The isolated spinal segments were fixed in 4% paraformaldehyde (Fisher Scientific) for 24 h at 4°C and transferred in a phosphate buffer solution (0.1 M) containing 0.9% of NaCl (PBS, pH = 7.4) containing 4% (wt/vol) of paraformaldehyde (PFA 4%). Then, the brains were incubated in a PBS solution containing 20% (wt/vol) sucrose for 24 h. For histology, brains were snap frozen in 2-methylbutane ($-45°C \pm 5°C$) and kept at $-80°C$ until immunofluorescence experiments were carried out. The procedures were similar to those used previously in lampreys, salamanders, and rats (Ryczko et al. 2013, 2015, 2016a, 2016b, 2017). All steps were carried out at room temperature unless stated otherwise. Floating 40-μm-thick coronal sections were collected at $-20°C$ using a cryostat (Leica CM 1860 UV). The sections were rinsed three times during 10 min in PBS and incubated during 1 h in a blocking solution containing 5% (vol/vol) of normal donkey serum and 0.3% Triton X-100 in PBS. The sections were incubated at 4°C for 48 h and agitated with an orbital shaker (40 rpm) in a PBS solution containing the primary antibody against choline acetyltransferase (ChAT) [goat anti-ChAT, Millipore AB144P, lot 3018862 (1:100) research resource identifier (RRID): AB_2079751], glutamate [rabbit anti-glutamate, Sigma G6642, lot 079M4802V (1:6,000), RRID AB_259946], Islet-1 and Islet-2 homeobox (Islet1/2) [mouse anti-Islet-1/2, Developmental Studies Hybridoma Bank (DSBH) 39.4D5, lot 1ea-24 μg/mL (1:100), RRID AB_2314683], vesicular glutamatergic transporter 2 (Vglut2) [mouse anti-Vglut2, Abcam AB79157, lots GR3197420-2 and GR331581-1 (1:500), RRID: AB_1603114], or 5-HT [rabbit anti-5-HT, Sigma S5545, lot 088M4835V (1:4,000) RRID: AB_477522]. Then, the sections were washed three times in PBS and incubated for 4 h in a solution containing the appropriate secondary antibody to reveal either 5-HT [donkey anti-rabbit Alexa Fluor 594, Invitrogen A21207 lot 1890862 (1:400), RRID: AB_141637], ChAT [donkey anti-goat Alexa Fluor 647, Invitrogen A21447, lot 1977345 (1:400), RRID: AB_141844], Islet1/2 or Vglut2 [donkey anti-mouse Alexa Fluor 488, Invitrogen A-21202 lot 1915874 (1:400), RRID AB_141607], and glutamate [donkey anti-mouse Alexa Fluor 594, Invitrogen A-21203, lot 2069656 (1:400), RRID AB_141633]. The slices were then rinsed three times in PBS for 10 min and mounted on Colorfrost Plus (Fisher) with a medium with DAPI (Vectashield H-1200), covered with a 1.5 type glass coverslip, and stored at 4°C before observation.

Epifluorescent and confocal microscopy. Brain sections were first observed using an epifluorescent microscope (Zeiss AxioImager M2 bundled with StereoInvestigator 2018 software v1.1, MBF Biosci-

ence) and objectives ($\times10$, $\times20$, $\times40$). Composite images were assembled from $\times20$ images using StereoInvestigator. Representative regions containing the cells or fibers of interest were photographed at higher magnification ($\times20$ or $\times40$). In some cases, confocal images were taken using a Leica TCS SP8 nanoscope bundled with LASX software (Leica). For confocal stacks, we used a $\times40$ objective, $1,024\times1,024$ pixel resolution (581.25 $\times$ 581.25 μm), 3 frames averaging, bidirectional scanning at 400-Hz speed and pinhole opened at 95.5 μm. The number of images taken for a stack varied from 38 to 136, the step between two images varied between 0.25 to 0.35 μm, and the total depth acquired varied from 13.1 to 34.0 μm. Contrast levels were adjusted so that all fluorophores were visible simultaneously, and digital images were merged using Photoshop CS6 (Adobe).

5-HT cell reconstructions. Confocal images of 5-HT immunoreactive cells were taken with a $\times40$ objective on the Leica TCS SP8 nanoscope and reconstructed using Neurolucida 360 (2018.1.1, MBF Bioscience) (Dickstein et al. 2016). The skeleton of the 5-HT neurons was first reconstructed in 3D automatically using the voxel scooping algorithm (Rodriguez et al. 2009). To refine the tracing, we used the interactive rayburst crawl algorithm to remove or add neurite segments based on careful 3D examination of the neuron (Xiao et al. 2018). The reconstructed cell was used to obtain a 2D projection and the soma was drawn using the tracing neuron function. Neurolucida Explorer was used to extract the morphometric parameters for each cell, including cell body area (μm^2), cell body perimeter (μm), neurite total length (μm), length per neurite (μm), and neurite diameter (μm). To evaluate the complexity of cell branching, a Sholl analysis (Sholl 1953) was carried out for each cell by quantifying the number of intersections between the neurites and spheres of increasing radius (step increase: 10 μm) centered on the cell body.

Specificity of the primary antibodies. The S5545 anti-5-HT antibody (Table 1) has been used by others to label spinal 5-HT neurons in the zebrafish spinal cord (Berg et al. 2018; Montgomery et al. 2018; Pedroni and Ampatzis 2019), rat spinal cord (Fouad et al. 2010), or rat brainstem (Ribas-Salgueiro et al. 2005). According to the manufacturer's datasheet, this whole antiserum does not cross-react with L-tryptophan, 5-hydroxytryptophan, *N*-acetyl-5-hydroxytryptamine, or dopamine. The manufacturer also reports that the staining is inhibited by preincubation with 5-HT. Staining and 5-HT brain content measured using HPLC are both largely reduced in known 5-HT regions following central depletion of 5-HT with p-chlorophenylalanine treatment in rats (Kornum et al. 2006).

The AB144P goat anti-ChAT antibody (Table 1) has been extensively used to label cholinergic neurons in salamanders (Cabelguen et al. 2003; Marín et al. 1997; Ryczko et al. 2016a, 2016b), lampreys (Le Ray et al. 2003; Quinlan and Buchanan 2008; Pombal et al. 2001; Ryczko et al. 2013), and humans (Massouh et al. 2008; Ryczko et al. 2016b). It stains motoneurons in zebrafish (Ohnmacht et al. 2016; Reimer et al. 2008). According to the manufacturer datasheet, the antibody was raised against human placental choline acetyltransferase and Western blot of brain cell lysates revealed that it labels a 68- to 70-kDA band corresponding to ChAT. It stains neurons expressing a green fluorescent protein under control of the ChAT promoter, e.g., in the basal forebrain (Bloem et al. 2014), septum (Blusztajn and Rinnofner 2016), and supraoptic nucleus (Wang et al. 2015).

The DSBH 39.4D5 supernatant (Table 1) was successfully used to label Islet-1/2, a well-established marker of motoneuron identity (Ericson et al. 1992; Hutchinson and Eisen 2006; Tsuchida et al. 1994). It has been used to label motoneurons in salamanders (Moreno and González 2007; Moreno et al. 2018) and in zebrafish (Hutchinson and Eisen 2006) as well as in chickens, mice, and rats (Yamamoto and Henderson 1999). The antibody detects Islet-1 and Islet-2 (Islet-1/2) proteins, and this is consistent with the patterns of mRNA labeling using in situ hybridization (Hutchinson and Eisen 2006). Additionally, Western blots showed that this antibody labels the Islet-1 protein proportionally with the level of *Islet-1* mRNA quantified with RT-PCR (Liu et al. 2011).

Table 1. *Primary antibodies*

Antigen	Catalog	Host	Incubation	Provider	RRID
ChAT (human placental enzyme)	AB144P	Goat	1:100, 48 h, 4°C	EMD Millipore, Billerica, MA	AB_2079751
Glutamate (L-glutamate conjugated to KLH)	G6642	Rabbit	1:6,000, 48 h, 4°C	Sigma, Saint Louis, MO	AB_259946
5-HT (serotonin creatinine sulfate complex conjugated to BSA)	S5545	Rabbit	1:4,000 48 h, 4°C	Sigma, Saint Louis, MO	AB_477522
Islet-1/2 (rat Islet-1 and Islet-2 homeobox)	39.4D5	Mouse	1:100, 48 h, 4°C	Developmental Studies Hybridoma Bank (DSBH)	AB_2314683
Vglut2 (recombinant full-length protein corresponding to rat Vglut2)	AB79157 clone [8G9.2]	Mouse	1:500, 48 h, 4°C	Abcam Inc, Ontario, Canada	AB_1603114

BSA, bovine serum albumin, ChAT, choline acetyltransferase; 5-HT, serotonin; KLH, keyhole limpet hemocyanin; RRID, research resource identifier; Vglut2, vesicular glutamate transporter 2.

The AB79157 anti-Vglut2 purified monoclonal antibody [clone 8G9.2] (Table 1) was successfully used to label the well-known glutamatergic pyramidal neurons in human brains (Gavin et al. 2012), glutamatergic neurons in rat dorsal root ganglia (Tang et al. 2020), cortical glutamatergic neurons in mice (Verma et al. 2015), and other known glutamatergic regions in the brain and spinal cord according to the manufacturer. Western blots carried out by the manufacturer show a band around 60 kDA, and this band is lost in *Vglut2* knockout mice (He et al. 2012). Dot-blot immunoassays validated the specificity of this antibody toward the Vglut2 protein in lysates of cortical neurons shown to express *Vglut2* RNA using RT-PCR (Verma et al. 2015). Immunolabeling with this antibody was used to show a decrease in Vglut2 expression following short hairpin RNA knockdown of Vglut2 in cultures of mouse brainstem neurons, and such a decrease was associated with reduced glutamatergic excitatory postsynaptic responses recorded with patch-clamp electrodes (Dimitrov et al. 2016). Vglut2 immunolabeling with the AB79157 antibody is consistent with the distribution of Vglut2 mRNA as shown by in situ hybridization and single-cell RNA sequencing in the subiculum region of the hippocampus in mice (Cembrowski et al. 2018).

The G6642 anti-glutamate polyclonal antibody (Table 1) was previously used to specifically label glutamatergic neurons in photoreceptor cells in the mouse retina (Terada et al. 2009), rat brainstem (Fredrich et al. 2009; Liang et al. 2014; Lin et al. 2000), zebrafish spinal cord (Pedroni and Ampatzis 2019), and mouse amygdala (Xu et al. 2015). Dot-blot immunoassays carried out by the manufacturer indicate that this antiserum recognizes L-glutamate, glutamate conjugated to keyhole limpet hemocyanin, glutamate conjugated to bovine serum albumin, and keyhole limpet hemocyanin. The manufacturer reports that this antiserum does not cross-react with L-aspartate, L-glutamine, L-asparagine, L-alanine, or bovine serum albumin and weakly cross-reacts with glycyl-L-aspartic acid, GABA, β-alanine, glycine, and 5-aminovaleric acid (see also Terada et al. 2009). Preincubation with glutamate eliminates labeling in zebrafish (Berg et al. 2018). The antiserum specifically labels zebrafish neurons expressing a fluorescent protein under control of the vglut2 promoter or under control of the Chx10 promoter (Pedroni and Ampatzis 2019), the latter being a population of spinal glutamatergic interneurons contributing to generate the locomotor rhythm from fish to mammals (V2a neurons; for review, see Kiehn 2016). For all the immunofluorescence experiments carried out in the present study, omitting the primary antibody from our procedures resulted in absence of labeling.

Statistical analysis. Data are presented as mean ± standard deviation (SD). No statistical method was used to predetermine sample sizes. Sample sizes are similar to those used in the field. No randomization or blinding procedure was used. Statistical analyses and graphs were done using SigmaPlot 12.0 (Systat). Parametric analyses were used when assumptions for normality (Shapiro–Wilk test) and equal variance (Levene's test) were respected; otherwise nonparametric analyses on ranks were used. To compare dependent groups, we used a parametric one-way repeated-measures analysis of variance (ANOVA) followed by Student–Newman–Keuls or a Fisher LSD post hoc tests. Statistical differences were considered to be significant when $P < 0.05$.

Data availability. All relevant data are within the paper and the numerical values underlying the figures are available on Figshare (doi: 10.6084/m9.figshare.12401318).

RESULTS

Citalopram destabilizes axial fictive locomotor activity. Rhythmic motor activities were generated in isolated spinal cords by bath applying the glutamatergic agonists NMDA (20 μM) and D-serine (10 μM). The evoked activities were recorded from axial VR6 to VR13 that innervate the trunk muscles (Francis 1934). The activities evoked in such preparations consist of left-right alternating bursts of motoneuron activities together with waves of intersegmental activity propagated rostrally or caudally (Delvolvé et al. 1999; Ryczko et al. 2010, 2015). The range of rhythm frequencies (0.05 to 0.17 Hz) and axial phase lags (−9.5 to 14.0% per segment, $n = 21$ preparations) were similar to those previously reported (Delvolvé et al. 1999; Ryczko et al. 2010, 2015). Wavelet transformations coupled with statistical analysis (Mor and Lev-Tov 2007) were used to evaluate the stability of the evoked activity over time before 5-HT drug application as previously done in such preparations (Ryczko et al. 2015). Stable cross-power and phase relationships were found between the wavelet transformations of ipsilateral (right side) VR recorded over relatively long bouts of fictive locomotion (~5 min) as previously reported (e.g., Fig. 1D; see Knüsel et al. 2013; Ryczko et al. 2015).

To evaluate the effect of endogenous serotonin on fictive locomotor activity, the SSRI citalopram was added to the bath at gradually increasing concentrations (0.1, 1, 2.5, and 5 μM; 30 min application for each concentration) (Fig. 1, A–C) and wavelet analysis was performed (Fig. 1, D–F). Cross-power was decreased at 1, 2.5, and 5 μM of citalopram ($P < 0.05$ versus control in each case, Student–Newman–Keuls test after a significant ANOVA for repeated measures on ranks $P < 0.05$, $n = 8$ to 10 animals per citalopram concentration) (Fig. 1H). Rhythm coherence was decreased at 2.5 and 5 μM of citalopram ($P < 0.001$ versus control in both cases, Student–Newman–Keuls test after a $P < 0.01$ ANOVA for repeated measures, $n = 8$ to 10 animals) (Fig. 1I). The amplitude of this deleterious effect on rhythm
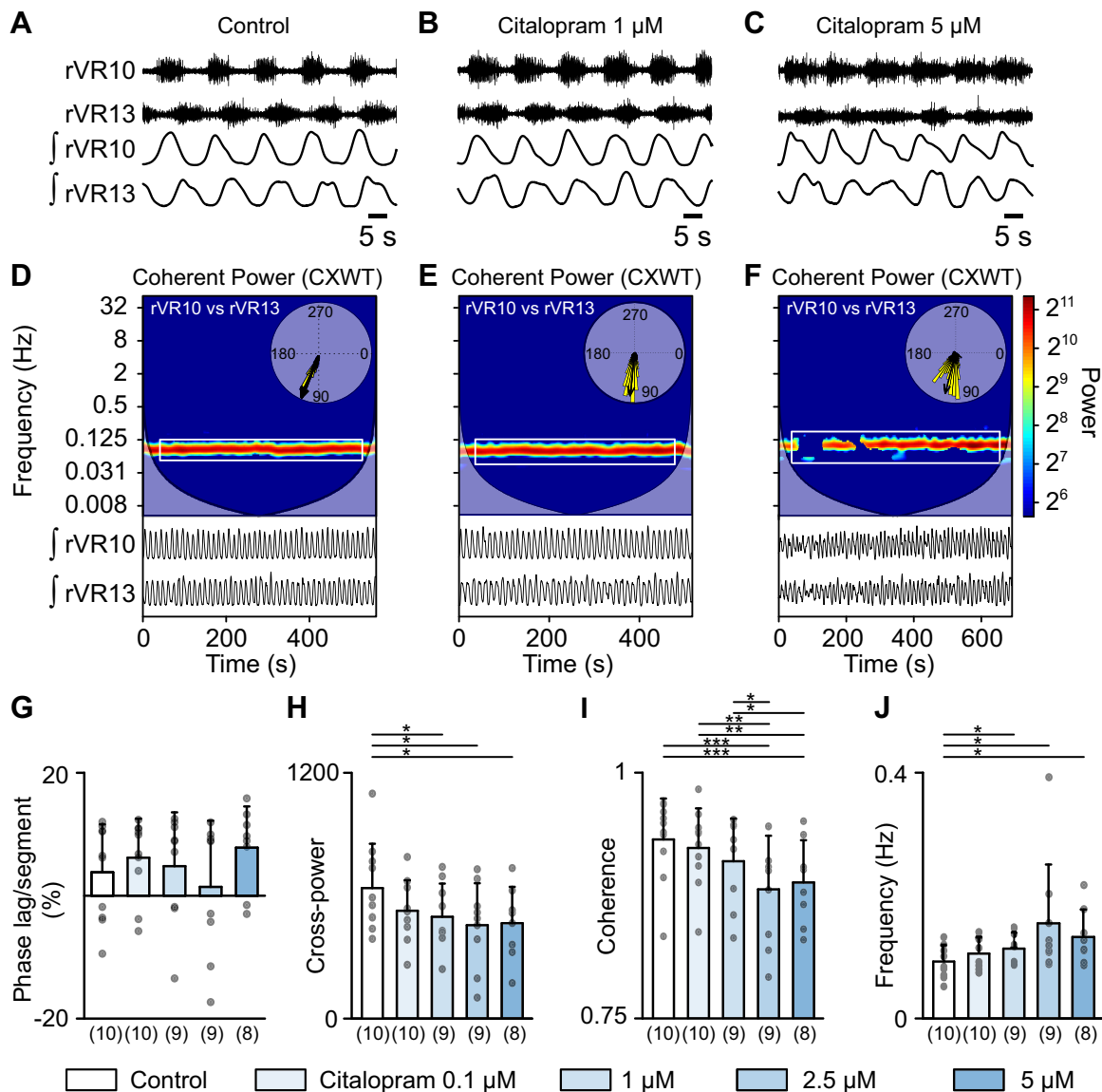
Fig. 1. Effects of the selective serotonin reuptake inhibitor citalopram on axial fictive locomotor activity. *A–C*: fictive locomotor activity evoked by bath application of the glutamatergic agonists *N*-methyl-D-aspartate (NMDA; 20 μM) and D-serine (10 μM) on isolated spinal cord preparations. Typical extracellular recordings obtained from ventral roots (VR) located on the right (r) side of spinal segments 10 and 13 (i.e., innervating trunk muscles) using suction electrodes. The traces were rectified and smoothed ($\int$ traces; see MATERIALS AND METHODS). After the control period, increasing concentrations of citalopram were applied each 30 min. *D* and *E*: coherent cross-power representation (CXWT; see Mor and Lev-Tov 2007) illustrating in time-frequency domains the coordination of the motor activities recorded from the two VRs. The analysis was performed on longer bouts of activities from the preparation illustrated in *A–C*. The frequency domain showing high cross-power (color coded) in close neighborhood of the locomotor rhythm was delineated (solid rectangle) for analysis in *G–J*. In the *insets*, the phase relationships (degrees) between the rhythmic activities of the two VRs are illustrated with vectors on circular plots. The mean vector was used to determine the corresponding intersegmental phase lag. *G–J*: effects of increasing concentrations of citalopram on the intersegmental phase lag (*G*), cross-power (*H*), rhythm coherence (*I*), and rhythm frequency (*J*). The number of animals is indicated in parentheses. Note that in some animals some concentrations of citalopram were not applied. Each gray dot represents one animal. Data from *A–F* were obtained from the same animal. *$P < 0.05$, **$P < 0.01$, ***$P < 0.001$, Student–Newman–Keuls post hoc test after a significant one-way ANOVA for repeated measures ($P < 0.05$ for *H*, $P < 0.01$ for *I*, $P < 0.001$ for *J*).

coherence increased with the concentration of citalopram applied (Fig. 1*I*). The reduction of rhythm coherence occurred together with an increase in rhythm frequency at 1, 2.5, and 5 μM of citalopram ($P < 0.05$ versus control in both cases, Student–Newman–Keuls test after a $P < 0.001$ ANOVA for repeated measures on ranks, $n = 8$ to 10 animals) (Fig. 1*J*). In contrast, we found no significant modification of phase relationships between ipsilateral VRs (ANOVA for repeated measures on ranks $P > 0.05$) (Fig. 1*G*). Altogether this indicated that citalopram destabilized the fictive locomotor rhythm.

The 5-HT$_{1A}$ antagonist WAY-100635 prevents citalopram-induced destabilization of fictive locomotor activity. We investigated whether the 5-HT$_{1A}$ receptor subtype could be involved in such deleterious effects, since their activation depresses fictive locomotion in mice (Dunbar et al. 2010) and depresses fictive scratching in turtles (Perrier et al. 2018) through a decrease in motoneuron excitability (Cotel et al. 2013). The 5-HT$_{1A}$ antagonist WAY-100635 (1 μM) was bath applied (30 min) during fictive locomotion (Fig. 2, *A–F*). The antagonist significantly increased rhythm coherence ($P < 0.05$ versus
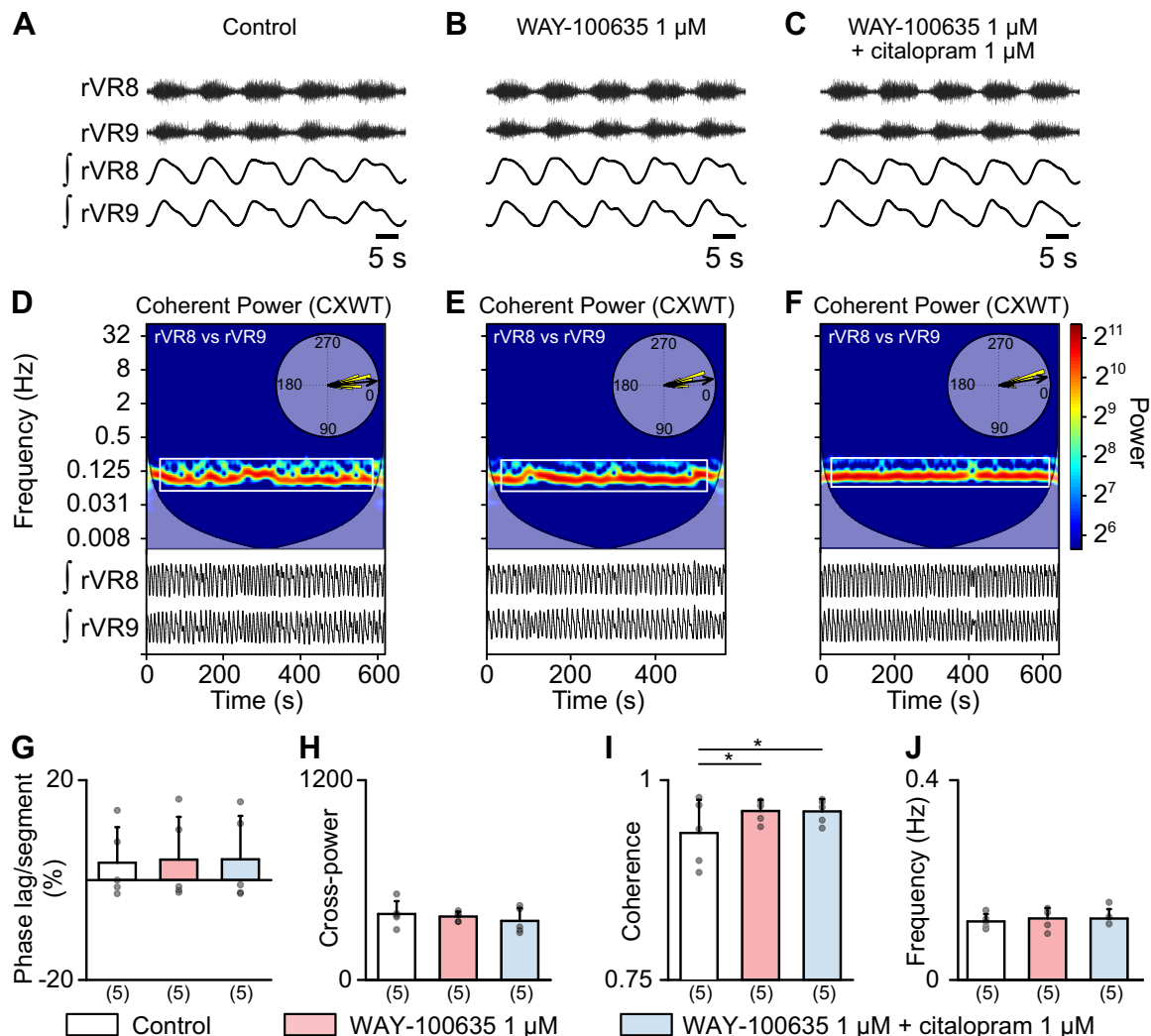
Fig. 2. Effects of the 5-HT$_{1A}$ antagonist WAY-100635 on axial fictive locomotor activity. *A–C*: fictive locomotor activity evoked by bath application of *N*-methyl-D-aspartate (NMDA; 20 μM) and D-serine (10 μM) on isolated spinal cord preparations. Typical extracellular recordings obtained from ventral roots (VR) located on the right (r) side of spinal segments 8 and 9 (i.e., innervating trunk muscles) using suction electrodes. The traces were rectified and smoothed ($\int$ traces; see MATERIALS AND METHODS). After the control period, the 5-HT$_{1A}$ antagonist WAY-100635 (1 μM) was applied during 30 min, then the selective serotonin reuptake inhibitor citalopram (1 μM) was added during 30 min. *D–F*: coherent cross-power representation (CXWT; see Mor and Lev-Tov 2007) illustrating in time-frequency domains the coordination of the motor activities recorded from the two VRs. The analysis was performed on longer bouts of activities from the preparation illustrated in *A–C*. The frequency domain showing high cross-power (color coded) in close neighborhood of the locomotor rhythm was delineated (solid rectangle) for analysis in *G–J*. In the *insets*, the phase relationships (degrees) between the rhythmic activities of the two VRs are illustrated with vectors on circular plots. The mean vector was used to determine the corresponding intersegmental phase lag. *G–J*: effects of drug applications on the intersegmental phase lag (*G*), cross-power (*H*), rhythm coherence (*I*), and rhythm frequency (*J*). The number of animals is indicated in parentheses. Each gray dot represents one animal. Data from *A–F* were obtained from the same animal. *$P < 0.05$, Fisher LSD post hoc test after a one-way ANOVA for repeated measures ($P < 0.05$ in *I*).

control, after a $P < 0.05$ ANOVA for repeated measures, $n = 5$ animals) (Fig. 2*I*) without affecting the other parameters (Fig. 2, *G*, *H*, and *J*). This suggests that an endogenous release of 5-HT recruits 5-HT$_{1A}$ receptors in control conditions. Addition of citalopram (1 μM) to the bath did not change intersegmental phase lag, rhythm coherence, rhythm frequency, or cross-power ($n = 5$ animals, Fig. 2, *G–J*). Altogether this suggests that activation of 5-HT$_{1A}$ receptors plays a role in the deleterious effects evoked by citalopram on fictive locomotion.

The 5-HT$_{1A/7}$ agonist 8-OH-DPAT destabilizes axial fictive locomotor activity. We then examined whether 5-HT$_{1A/7}$ receptor activation could mimic some of the deleterious effects of citalopram (Fig. 3, *A–D*). Bath-application of the 5-HT$_{1A/7}$ agonist 8-OH-DPAT at 0.1 and 1 μM (30 min for each concentration) significantly decreased rhythm coherence at 1

μM ($P < 0.05$ versus control, after a $P < 0.05$ ANOVA for repeated measures, $n = 6$ animals) (Fig. 3*G*). This effect was associated with a decrease in intersegmental phase lag ($P < 0.05$ versus control, after a $P < 0.05$ ANOVA for repeated measures, $n = 6$ animals) (Fig. 3*E*). We observed no significant modification of cross-power (Fig. 3*F*) or rhythm frequency (Fig. 3*H*). This indicated that activation of 5-HT$_{1A/7}$ receptors is sufficient to destabilize fictive locomotor activity.

5-HT fibers and cell bodies in the axial spinal cord. We then examined the possible substrate of these effects using immunofluorescence experiments against 5-HT in axial spinal segments of salamanders. We found 5-HT-positive fibers and cell bodies in axial segments as previously reported (Branchereau et al. 2000; Jovanović et al. 1996; Sims 1977) (Fig. 4, *A–J*). 5-HT-positive cell bodies were located medioventrally, some-
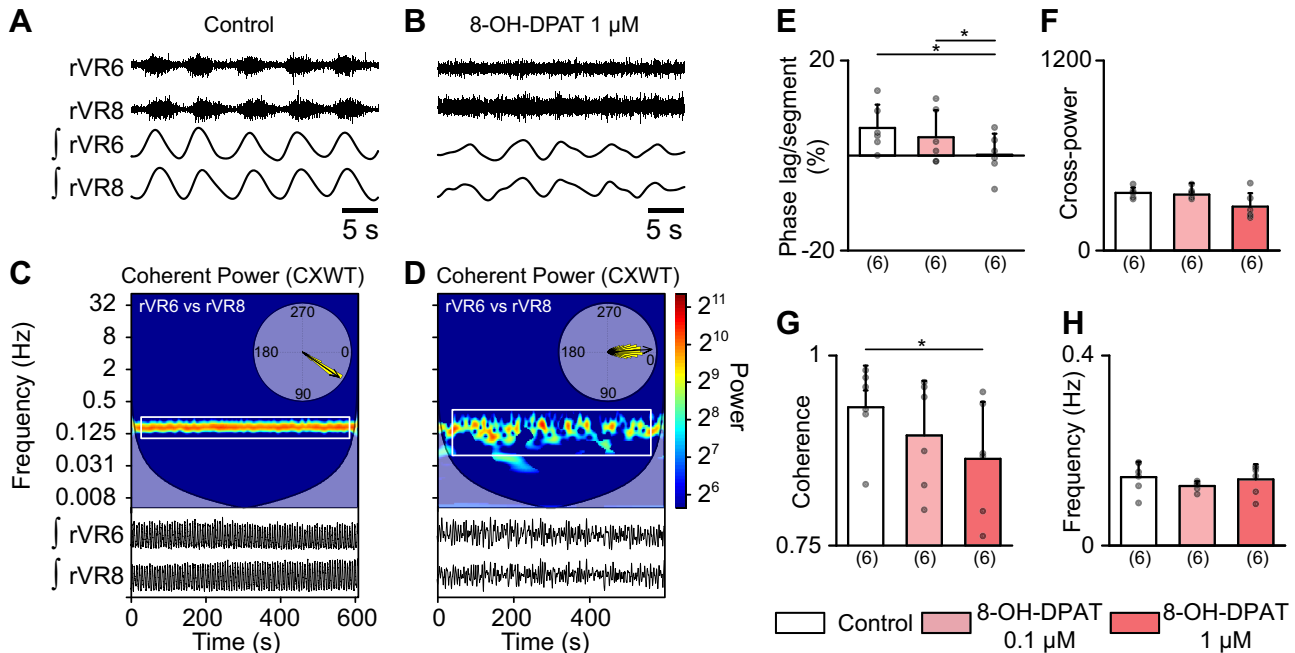
Fig. 3. Effects of the 5-HT$_{1A/7}$ agonist 8-OH-DPAT on axial fictive locomotor activity. *A* and *B*: fictive locomotor activity evoked by bath application of *N*-methyl-D-aspartate (NMDA; 20 μM) and D-serine (10 μM) on isolated spinal cord preparations in control conditions and in presence of the 5-HT$_{1A/7}$ agonist 8-OH-DPAT. Typical extracellular recordings obtained from ventral roots (VR) located on the right (r) side of spinal segments 6 and 8 (i.e., innervating trunk muscles) using suction electrodes. The traces were rectified and smoothed ($\int$ traces; see MATERIALS AND METHODS). After the control period, the 5-HT$_{1A/7}$ agonist 8-OH-DPAT was applied during 30 min at 0.1 μM, and then during 30 min at 1 μM. *C* and *D*: coherent cross-power representation (CXWT; see Mor and Lev-Tov 2007) illustrating in time-frequency domains the coordination of the motor activities recorded from the two VRs. The analysis was performed on longer bouts of activities from the preparation illustrated in *A* and *B*. The frequency domain showing high cross-power (color coded) in close neighborhood of the locomotor rhythm was delineated (solid rectangle) for analysis in *E–H*. In the *insets*, the phase relationships (degrees) between the rhythmic activities of the two VRs are illustrated with vectors on circular plots. The mean vector was used to determine the corresponding intersegmental phase lag. *E–H*: effects of increasing concentrations of the 5-HT$_{1A/7}$ agonist 8-OH-DPAT on the intersegmental phase lag (*E*), cross-power (*F*), rhythm coherence (*G*), and rhythm frequency (*H*). The number of animals is indicated in parentheses. Each gray dot represents one animal. Data from *A–D* were obtained from the same animal. *$P < 0.05$, Student–Newman–Keuls post hoc test after a significant one-way ANOVA for repeated measures ($P < 0.05$ both in *E* and *G*).

times in small clusters of two or three that send projections onto each other (Fig. 4, *C, E–G*). In the axial segment 9, we found 7 ± 4 5-HT-immunoreactive cell bodies (*n* = 3 segments from *n* = 3 animals). 5-HT-immunoreactive fibers and varicosities were consistently distributed throughout the whole section of the spinal cord, except for the dorsomedial region that was less labeled (Fig. 4, *A* and *B*). Some of these fibers appeared to originate from spinal 5-HT neurons, which overall had a low number of neurites and a limited level of complexity as shown by cell reconstructions (Fig. 4, *H–M*) and morphometric measurements (Fig. 4, *N–S*). Occasionally neurites bifurcated toward the central canal, but more often were oriented ventrolaterally (Fig. 4, *B–D*) where a very dense immunopositive 5-HT plexus was located at the border between the spinal cord and the meninges (Fig. 4*D*).

5-HT innervation of motoneurons. We next examined whether ventral neurons of the axial spinal cord were innervated by 5-HT fibers. Putative motoneurons were labeled using immunofluorescence against choline acetyltransferase (ChAT) (Chevallier et al. 2006, 2008). These neurons were mostly located in the ventrolateral region (*n* = 3 animals, Fig. 5*A*). In double-labeling experiments, we found that many ChAT-positive neurons were also positive for the motoneuron marker Islet-1/2 (*n* = 3 animals, Fig. 5, *C–E* and *F–H*). We found 5-HT fibers and varicosities in close apposition with the cell bodies of ChAT-positive cells (*n* = 3 animals, Fig. 5, *A* and *B*, *I–K*). Triple-labeling experiments indicated that 5-HT-immu-

noreactive fibers and varicosities were in close apposition with cell bodies of motoneurons positive both for ChAT and Islet-1/2 (*n* = 2 animals, Fig. 5, *L–O*).

5-HT innervation of ventral glutamatergic neurons. As in other vertebrates, the axial fictive locomotor rhythm relies on synaptic glutamatergic transmission in salamanders (Bicanski et al. 2013; Ryczko et al. 2010). The effects of citalopram recorded above suggest that glutamatergic neurons could be a relevant target for 5-HT modulation. Immunofluorescence experiments against glutamate (Ryczko et al. 2016a, 2016b) revealed an abundant population of positive neurons in axial spinal segments (Fig. 6, *A, C,* and *F, n* = 2 animals). We also found many neurons positive for Vglut2, a marker used to label some glutamatergic neurons in other species (Gavin et al. 2012; Tang et al. 2020; Verma et al. 2015) (Fig. 6, *B, D,* and *G, n* = 2 animals). This marker labels neurons that contribute to generate the locomotor rhythm in mammalian tetrapods (e.g., Hägglund et al. 2010, 2013). Using double-labeling experiments, we found that many glutamate-positive neurons were also positive for Vglut2 (Fig. 6, *C–E* and *F–H, n* = 2 animals). Among ventral neurons, which are more likely to be involved in motor control, 5-HT fibers and varicosities were found around Vglut2-positive cell bodies in axial segments innervating the trunk or tail (Fig. 6, *I–M, n* = 2 animals). Altogether these neuroanatomical results suggest that ventrally located populations of motoneurons and Vglut2-positive neurons are possible targets of 5-HT release in salamanders.

DISCUSSION

Our study shows that citalopram destabilized the fictive axial locomotor rhythm in isolated spinal cords. This was blocked by the 5-HT$_{1A}$ antagonist WAY-100635 and mimicked by the 5-HT$_{1A/7}$ agonist 8-OH-DPAT. A possible substrate for these effects was examined using immunofluorescence experiments in axial spinal segments. 5-HT fibers were found in close apposition with motoneurons immunopositive for ChAT and Islet-1/2 and in close apposition with Vglut2-positive ventral neurons, among which many were positive for glutamate.
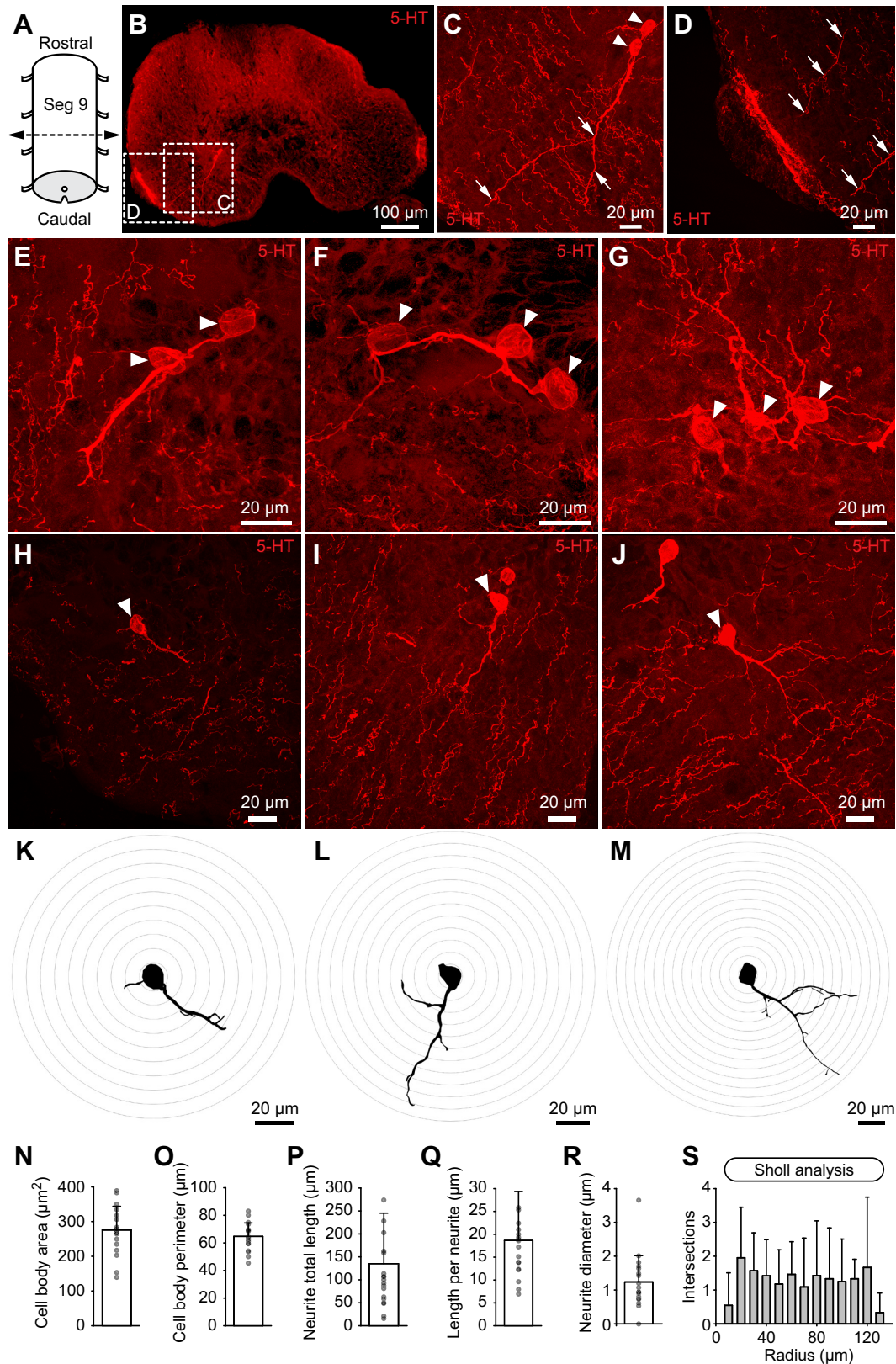
The spinal 5-HT system. Our data show that motoneurons and glutamatergic interneurons are possible targets for the release of endogenous 5-HT. The anatomy of the spinal 5-HT system reported here in the salamander *Ambystoma mexicanum* is strikingly identical to that reported in the salamander *Pleurodeles waltl* (Branchereau et al. 2000), which also possess ChAT-immunoreactive motoneurons (Chevallier et al. 2006, 2008) and glutamatergic neurons that contribute to rhythmic bursting in axial segments according to previous electrophysiological experiments (Ryczko et al. 2010). Although we cannot rule out the contrary, we suggest that the anatomical observations reported in *Ambystoma* should be relevant to interpret the effects of 5-HT drugs recorded in *Pleurodeles*.

The 5-HT system reported here is largely similar to that of other vertebrates. The spinal 5-HT fibers mostly originate from brainstem raphe neurons in salamander (Branchereau et al. 2000) as in lamprey (Zhang et al. 1996), turtle (Fabbiani et al. 2018) and mouse (Dunbar et al. 2010). Such descending 5-HT fibers modulate motoneuron excitability and rhythm generating circuits as well established, e.g., in turtles (Cotel et al. 2013; Perrier and Delgado-Lezama 2005; Perrier et al. 2018; for review, see Perrier and Cotel 2015). Intraspinal 5-HT neurons are also present in lamprey (Harris-Warrick et al. 1985; Van Dongen et al. 1985), zebrafish (Berg et al. 2018; McLean and Fetcho 2004), dogfish (Carrera et al. 2008), stingray (Ritchie and Leonard 1982), garfish (Parent and Northcutt 1982; Chiba 2007), turtle (Fabbiani et al. 2018), chick (Sako et al. 1986), mouse (Ballion et al. 2002), rat (Newton et al. 1986), and monkey (Lamotte et al. 1982). In our material, these neurons projected occasionally to the central canal, and more frequently to the ventrolateral 5-HT plexus as in *Pleurodeles* (Branchereau et al. 2000), lamprey (Harris-Warrick et al. 1985; Schotland et al. 1996; Van Dongen et al. 1985), garfish (Chiba 2007), stingray (Ritchie et al. 1984), sturgeon (Adrio et al. 1999), and dogfish (Carrera et al. 2008). The intraspinal 5-HT neurons were proposed to target at least in part locomotor interneurons and motoneurons in lamprey (Schotland et al. 1996; Van Dongen et al. 1985). The function of the plexus at the border of the spinal cord is not resolved but could play a role in paracrine release of 5-HT into the extraspinal space (Chiba 2007; Schotland et al. 1996).

Destabilization of locomotor activity. Our results are in accordance with studies reporting that citalopram depresses the fictive axial locomotor rhythm in almost half of lamprey spinal cords recorded (Christenson et al. 1989), depresses the fictive locomotor activity of limb networks in the mouse spinal cord (Dunbar et al. 2010), destabilizes the episodic organization of fictive locomotor bouts, and decreases the number of bursts in larval zebrafish (Montgomery et al. 2018). This is in line with results showing that optogenetic stimulation of 5-HT neurons/fibers (Pet1-positive) in the spinal cord decreases the number of fictive locomotor bursts in zebrafish (Montgomery et al.

2018). It is unclear whether this deleterious effect involves intraspinal 5-HT neurons or descending 5-HT fibers from the raphe, which both express Pet1 (Lillesaar et al. 2007; Montgomery et al. 2016; Yokogawa et al. 2012). Interestingly, prolonged stimulation of the raphe 5-HT fibers in the spinal cord depresses fictive scratching in turtle (Perrier et al. 2018). Altogether this indicates that increasing 5-HT release in the spinal cord has deleterious effects on motor pattern generation.

The 5-HT$_{1A}$-dependent deleterious effect that we report here is in accordance with a study in neonatal mice showing that 5-HT$_{1A}$ receptor activation is involved in the decreased stability evoked by citalopram during fictive locomotion (Dunbar et al. 2010). Similarly, 5-HT$_{1A}$ receptor activation deteriorates fictive locomotion in neonatal rats (Oueghlani et al. 2020). In turtles, stimulation of descending 5-HT fibers decreases the excitability of motoneurons through the activation of 5-HT$_{1A}$ receptors, which inhibit a Na$^+$ current involved in action potential generation (Cotel et al. 2013; Perrier and Cotel 2008; Perrier and Delgado-Lezama 2005). In humans, 5-HT$_{1A}$ receptor activation depresses motoneuron excitability (D'Amico et al. 2017, Kavanagh et al. 2019). Functionally, the 5-HT$_{1A}$-mediated inhibition of motoneurons was proposed to prevent muscle damage during intense activity (Cotel et al. 2013; D'Amico et al. 2017; Kavanagh et al. 2019; Perrier 2019) or to shift between motoneuron pools (Perrier and Cotel 2015; Perrier et al. 2018).

Our anatomical data suggest that 5-HT release targets motoneurons. 5-HT$_{1A}$ receptors are present in salamanders according to gene sequencing (Reyes-Ruiz et al. 2013) and electrophysiological data (Delay et al. 1997). In other tetrapods, 5-HT$_{1A}$ receptor mRNA is expressed in the dorsal and ventral horns of the spinal cord (mouse: Landry et al. 2006; rat: Croul et al. 1998; Thor et al. 1993) including motoneurons (rat: Woodrow et al. 2013). Our anatomical data also suggest that 5-HT release could target glutamatergic interneurons involved in axial rhythm generation. In lamprey, exogenous 5-HT reduces synapse strength from excitatory premotor neurons, commissural inhibitory neurons, and commissural excitatory neurons to motoneurons (e.g., Biró et al. 2006). In mouse, some of the excitatory neurons involved in locomotor rhythmogenesis are called V2a interneurons (Chx-10 positive, among which many are Vglut2 positive; Hägglund et al. 2010). Application of exogenous 5-HT onto these neurons increases cell excitability or evokes bistable properties (Dietz et al. 2012; Husch et al. 2012, 2015; Zhong et al. 2010). In addition, 5-HT also modulates calcium currents in mouse commissural interneurons (Abbinanti and Harris-Warrick 2012; Abbinanti et al. 2012; Díaz-Ríos et al. 2007). Altogether these data indicate that premotor neurons are targeted by 5-HT modulation from basal vertebrates to mammals. Single-cell recordings should be used in future studies to determine which cell populations are

Fig. 4. Serotoninergic (5-HT) neurons in the axial spinal cord. *A*: schematic representation of some axial salamander spinal segments. *B*: transverse section of axial spinal segment 9 (Seg 9) showing fibers and cell bodies positive for 5-HT (red). *C*: 5-HT-positive cells bodies (white arrowheads) were found on the ventral side of the spinal cord, with their fibers (white arrows) extending ventrolaterally, where the ventrolateral 5-HT-immunoreactive plexus (*D*) is located. Note the dense presence of 5-HT-positive fibers in the ventral part of the spinal cord in *C*. *D*: a dense plexus of 5-HT-positive fibers was consistently found at the border between the nervous system and the dura. Some 5-HT-positive fibers, likely originating from the 5-HT cell bodies, were pointing at the plexus (white arrows). Many other 5-HT fibers, likely from a different origin, were not pointing toward the plexus. *E–G*: clusters of 5-HT cell bodies (white arrowheads) located in the ventromedial region, likely sending projections to each other. *H–M*: three examples of 5-HT-positive neurons (*H–J*) and the corresponding 3D reconstructions that here appear projected in 2D (*K–M*). *N–S*: morphometric measurements obtained from 22 reconstructed cells obtained from three animals (3, 8, and 11 cells per animal). In *S*, the Sholl analysis gives an index of cell morphological complexity by quantifying the number of intersections between their neurites and spheres with increasing diameters centered on the cell body. Data from *B–M* were obtained from three animals.
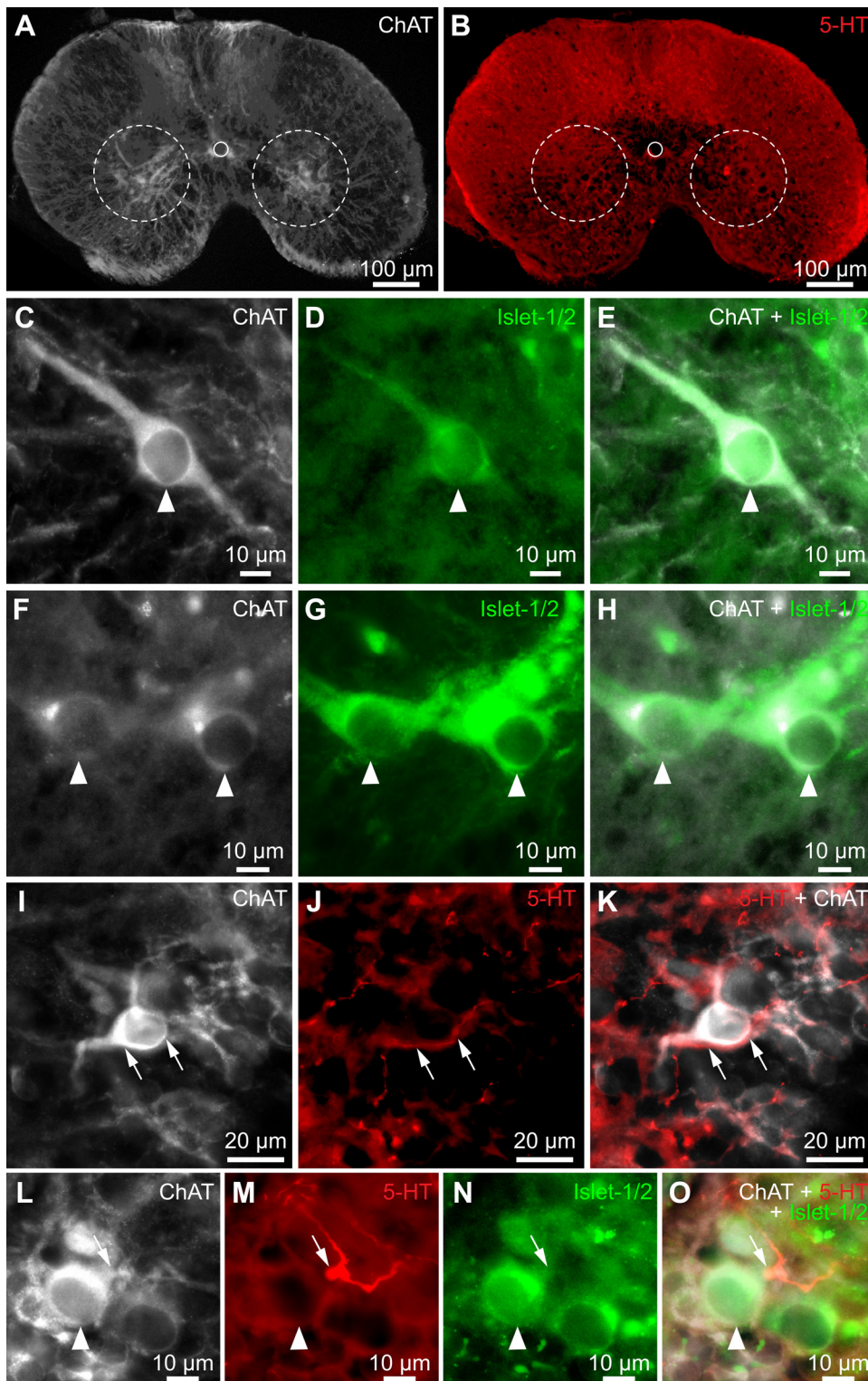
Fig. 5. Serotoninergic (5-HT) fibers in close apposition with motoneurons in the axial spinal cord. *A* and *B*: transverse section of axial spinal segment 9 showing fibers and cell bodies positive for choline acetyltransferase (ChAT, white, *A*) or 5-HT (red, *B*). The white dashed circles delineate the approximate position of the motoneurons. The white solid circles delineate the position of the central canal. *C–H*: two series of photomicrographs (*C–E*, *F–H*) showing examples of motoneurons (arrowheads) in the ventral spinal cord showing immunoreactivity for ChAT (white, *C* and *F*) and for the motoneuron marker Islet-1/2 (green, *D* and *G*), and the double labeling (*E* and *H*). *I–K*: photomicrographs showing a putative motoneuron (ChAT-positive, white, *I*) closely surrounded by a 5-HT-positive fiber (red, *J*) and the double labeling (*K*). *L–O*: triple-labeling experiment (*O*) showing a 5-HT-positive fiber and varicosity (red, *M*) in close apposition with a motoneuron cell body positive for ChAT (white, *L*) and Islet-1/2 (green, *N*). Data from *A–O* were obtained from three animals.

modulated by 5-HT in the spinal locomotor network of salamanders.

Rhythm frequency and phase lag. The citalopram-evoked increase in frequency reported here was unexpected, considering that exogenous 5-HT slows down the axial rhythm in a brainstem-spinal cord preparation of the same species (Branchereau et al. 2000). Some authors underlined that variable effects on motor output might not be surprising when manipulating pharmacologically the 5-HT system. Sharples and Whelan (2017) demonstrated in mice that the same neuromodulator can have divergent effects on the spinal locomotor network as a function of its excitability state, as shown in invertebrates (for review, see Marder et al. 2014). Perrier and Cotel (2015) proposed that exogenous versus endogenous 5-HT might differentially recruit synaptic versus extra synaptic "excitatory" (5-HT$_2$) or "inhibitory" (5-HT$_1$) receptors. This
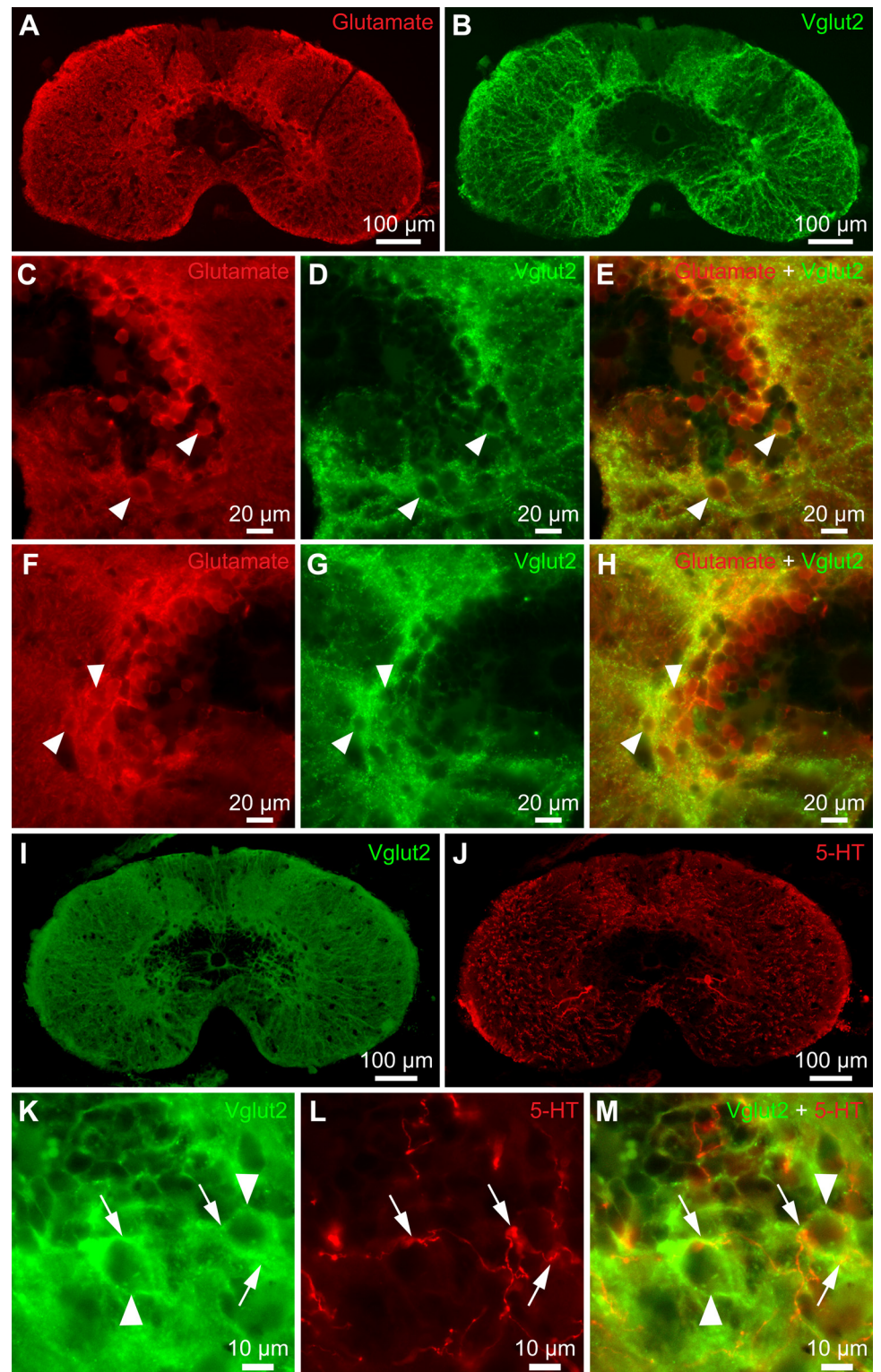
Fig. 6. Serotoninergic (5-HT) fibers in close apposition with glutamatergic neurons in the axial spinal cord. *A* and *B*: transverse section of axial spinal segment 11 showing cell bodies positive for glutamate (red, *A*) or the vesicular glutamatergic transporter (Vglut2, green, *B*). *C–H*: two series of photomicrographs (*C–E, F–H*) showing examples of neurons (arrowheads) immunoreactive for glutamate (red, *C* and *F*) and Vglut2 (green, *D* and *G*), and the double labeling (*E* and *H*). *I* and *J*: transverse section of axial spinal segment 9 showing fibers and cell bodies positive for Vglut2 (green, *I*) and fibers and varicosities positive for serotonin (red, *J*). *K–M*: photomicrographs showing Vglut2-positive neurons (green, *K*) closely surrounded by 5-HT-positive fibers and varicosities (red, *L*), and the double labeling (*M*). Data from *A–M* were obtained from two animals.

could explain a similar paradox reported in frog embryos, where exogenous 5-HT decreased rhythm frequency whereas the SSRI clomipramine increased rhythm frequency (McLean and Sillar 2004). However, such differences between exogenous and endogenous 5-HT are not systematically observed, e.g., in a salamander limb preparation with sensory feedback intact, both 5-HT and the SSRI zimelidine slow down the rhythm (*Necturus maculatus*, Jovanović et al. 1996). In rats,

exogenous 5-HT was reported to slow down (Beato and Nistri 1998; Madriaga et al. 2004; Pearlstein et al. 2005; Sqalli-Houssaini et al. 1993) or speed up the rhythm (Cazalets et al. 1992). Less variability was reported in lamprey, where a slowdown of the fictive rhythm was evoked in most studies when applying exogenous 5-HT (e.g., Harris-Warrick and Cohen 1985; Matsushima and Grillner 1992) or citalopram (Christenson et al. 1989), although inconsistent effects were

also reported with citalopram (Matsushima and Grillner 1992). In zebrafish, a slowdown was reported with exogenous 5-HT as with citalopram (Gabriel et al. 2009), whereas no effect on swimming but a reduction of inactivity periods was reported when applying exogenous 5-HT in agarose-embedded larval zebrafish (Brustein et al. 2003). In mice, a slowdown of the fictive locomotor rhythm was observed with citalopram but only if the brainstem was connected to the spinal cord (Dunbar et al. 2010). To what extent the presence of the brainstem plays a role in the effects of citalopram in salamanders remains to be determined.

In our study, 5-HT$_{1A}$ receptors appear to play a role in the effects of citalopram on frequency. The citalopram-evoked increase in frequency occurred together with a decrease in rhythm coherence, and both effects were blocked by a 5-HT$_{1A}$ receptor antagonist. The role of 5-HT$_{1A}$ receptors on rhythm frequency is not fully clear from our results, since the 5-HT$_{1A/7}$ agonist only decreased rhythm stability without increasing rhythm frequency. The 5-HT$_{1A/7}$ agonist also destabilized intersegmental phase lag, whereas citalopram or the 5-HT$_{1A}$ antagonist did not have any effect on intersegmental phase lag. The respective roles of 5-HT$_7$ and 5-HT$_{1A}$ receptors remain to be examined by future studies. In lamprey, several studies have reported modulation of the intersegmental phase lag with exogenous 5-HT (prolongation of the phase lag, e.g., Harris-Warrick and Cohen 1985; Matsushima and Grillner 1992) or endogenous 5-HT (prolongation; Christenson et al. 1989; Matsushima and Grillner 1992). The cellular mechanisms involved in the modulation of rhythm frequency and phase lag by 5-HT$_{1A}$ receptors remain to be examined in salamanders. In lamprey, 5-HT$_{1A}$-dependent mechanisms comprise a reduction of the after hyperpolarisation (Wikström et al. 1995) or a reduction of the postinhibitory rebound in commissural interneurons (Wang et al. 2011). We can speculate that 5-HT could have different effects depending on the cell population targeted by 5-HT release. In the lamprey spinal cord surgically deprived from the contralateral side (i.e., the hemicord), 5-HT increases rhythm speed (Cangiano and Grillner 2005), suggesting that such effects might occur without modulating commissural neurons. Although likely not involved in our study, presynaptic inhibition of transmitter release from reticulospinal neurons may also contribute to the effects of 5-HT as shown in lamprey (Buchanan and Grillner 1991; Gerachshenko et al. 2009; Photowala et al. 2006; Takahashi et al. 2001; for review, see Daghfous et al. 2016).

Pathological aspects. In the clinic, no beneficial effect of SSRIs was found on over ground and treadmill walking in humans with incomplete spinal cord injury, but rather a decrease in stride length was observed (Leech et al. 2014; Thompson and Hornby 2013). The SSRI citalopram increased strength but also spasticity in patients with spinal cord injury (D'Amico et al. 2013; Thompson and Hornby 2013) and increased spasticity after stroke (Gourab et al. 2015). These effects could involve 5-HT$_2$ receptor activation, which increases motoneuron firing in animal models (for review, see Perrier and Cotel 2015). In line with this, blockade of 5-HT$_2$ receptors decreases the spasms (D'Amico et al. 2013; Thompson and Hornby 2013). In intact human subjects, another SSRI (paroxetine) slightly increased the maximal voluntary contraction, an effect also proposed to involve 5-HT$_2$ receptors (Kavanagh et al. 2019). However, paroxetine also decreased their ability to perform sustained voluntary arm muscle contractions, suggesting a decrease in motoneuron excitability and a role for 5-HT in central fatigue (Kavanagh et al. 2019). The decrease in motoneuron excitability is believed to involve 5-HT$_{1A}$ receptors, since administration of the 5-HT$_{1A}$ agonist buspirone decreased motoneuron excitability in intact human subjects (D'Amico et al. 2017), building upon previous studies in animal models (Cotel et al. 2013; see Perrier 2019). The 5-HT$_{1A}$ receptors were found to be expressed in motoneurons in human lumbar segments (Perrin et al. 2011). Therefore, it may be important to take into account such possible deleterious effects when administrating SSRIs to patients with spinal cord injury treated for depression (Kemp and Krause 1999) or for motor recovery after stroke (Chollet et al. 2011; Dam et al. 1996).

Although 5-HT$_{1A/7}$ activation disrupts fictive rhythmic motor activity as reported here and elsewhere (e.g., Dunbar et al. 2010; Oueghlani et al. 2020; Perrier et al. 2018), administration of the 5-HT$_{1A/7}$ agonist 8-OH-DPAT alone or in combination with the 5-HT$_{2A}$ agonist quipazine promotes locomotor movements in vivo in animal models of spinal cord injury (Antri et al. 2003; Landry et al. 2006). Such beneficial effects on locomotor activity were potentiated when administered in combination with epidural stimulation of the spinal cord in rat models of spinal cord injury (Courtine et al. 2009; Gerasimenko et al. 2007; Musienko et al. 2011; van den Brand et al. 2012). It is likely that 5-HT$_{1A/7}$ agonists may also act at the level of spinal sensory inputs, which are known to play a key role in the reactivation of the central pattern generator for locomotion after spinal cord injury (Formento et al. 2018; Takeoka et al. 2014; for review, see e.g., Rossignol and Frigon 2011). The mRNA of 5-HT$_{1A}$ (Thor et al. 1993) and 5-HT$_7$ (Meuser et al. 2002) receptors are more densely expressed in the dorsal than in the ventral horn in rodents. The expression of 5-HT$_{1A}$ receptor increases in the dorsal horn after spinal cord injury (Otoshi et al. 2009). The beneficial effects of 5-HT$_{1A/7}$ receptor activation on locomotor activity were proposed to be independent from an effect in motoneurons in rats with spinal cord injury (Sławińska et al. 2014a; for review, see Sławińska et al. 2014b). Future studies should determine whether and how 5-HT$_{1A}$ receptor activation in spinal sensory circuits counteracts the deleterious effects of 5-HT$_{1A}$ receptor activation on motor pattern generation (present study; Dunbar et al. 2010; Perrier et al. 2018) and motoneuron excitability (Cotel et al. 2013; D'Amico et al. 2017; Perrier 2019), and how this evolves in spinal cord injury conditions.

DISCLOSURES

No conflicts of interest, financial or otherwise, are declared by the authors.

AUTHOR CONTRIBUTIONS

A.F., J.-M.C., and D.R. conceived and designed research; A.F., J.-M.C., and D.R. performed experiments; A.F. and D.R. analyzed data; A.F. and D.R. interpreted results of experiments; A.F. and D.R. prepared figures; D.R. drafted manuscript; A.F. and D.R. edited and revised manuscript; A.F. and D.R. approved final version of manuscript.

ENDNOTE

At the request of the authors, readers are herein alerted to the fact that additional materials related to this manuscript may be found at https://doi.org/10.6084/m9.figshare.12401318. These materials are not a part of this manuscript, and have not undergone peer review by the American Physiological Society (APS). APS and the journal editors take no responsibility for these materials, for the website address, or for any links to or from it.

REFERENCES

Abbinanti MD, Harris-Warrick RM. Serotonin modulates multiple calcium current subtypes in commissural interneurons of the neonatal mouse. *J Neurophysiol* 107: 2212–2219, 2012. doi:10.1152/jn.00768.2011.

Abbinanti MD, Zhong G, Harris-Warrick RM. Postnatal emergence of serotonin-induced plateau potentials in commissural interneurons of the mouse spinal cord. *J Neurophysiol* 108: 2191–2202, 2012. doi:10.1152/jn.00336.2012.

Adrio F, Anadón R, Rodríguez-Moldes I. Distribution of serotonin (5HT)-immunoreactive structures in the central nervous system of two chondrostean species (Acipenser baeri and Huso huso). *J Comp Neurol* 407: 333–348, 1999. doi:CO;2-R;/Border [0 0 0]?>10.1002/(SICI)1096-9861(19990510)407:3<333:AID-CNE3>3.0.CO;2-R.

Antri M, Mouffle C, Orsal D, Barthe J-Y. 5-HT1A receptors are involved in short- and long-term processes responsible for 5-HT-induced locomotor function recovery in chronic spinal rat. *Eur J Neurosci* 18: 1963–1972, 2003. doi:10.1046/j.1460-9568.2003.02916.x.

Ballion B, Branchereau P, Chapron J, Viala D. Ontogeny of descending serotonergic innervation and evidence for intraspinal 5-HT neurons in the mouse spinal cord. *Brain Res Dev Brain Res* 137: 81–88, 2002. doi:10.1016/S0165-3806(02)00414-5.

Beato M, Nistri A. Serotonin-induced inhibition of locomotor rhythm of the rat isolated spinal cord is mediated by the 5-HT1 receptor class. *Proc Biol Sci* 265: 2073–2080, 1998. doi:10.1098/rspb.1998.0542.

Beliez L, Barrière G, Bertrand SS, Cazalets J-R. Origin of thoracic spinal network activity during locomotor-like activity in the neonatal rat. *J Neurosci* 35: 6117–6130, 2015. doi:10.1523/JNEUROSCI.4145-14.2015.

Berg EM, Bertuzzi M, Ampatzis K. Complementary expression of calcium binding proteins delineates the functional organization of the locomotor network. *Brain Struct Funct* 223: 2181–2196, 2018. doi:10.1007/s00429-018-1622-4.

Bicanski A, Ryczko D, Cabelguen J-M, Ijspeert AJ. From lamprey to salamander: an exploratory modeling study on the architecture of the spinal locomotor networks in the salamander. *Biol Cybern* 107: 565–587, 2013. doi:10.1007/s00422-012-0538-y.

Biró Z, Hill RH, Grillner S. 5-HT modulation of identified segmental premotor interneurons in the lamprey spinal cord. *J Neurophysiol* 96: 931–935, 2006. doi:10.1152/jn.00309.2006.

Bloem B, Schoppink L, Rotaru DC, Faiz A, Hendriks P, Mansvelder HD, van de Berg WDJ, Wouterlood FG. Topographic mapping between basal forebrain cholinergic neurons and the medial prefrontal cortex in mice. *J Neurosci* 34: 16234–16246, 2014. doi:10.1523/JNEUROSCI.3011-14.2014.

Blusztajn JK, Rinnofner J. Intrinsic cholinergic neurons in the hippocampus: fact or artifact? *Front Synaptic Neurosci* 8: 6, 2016. doi:10.3389/fnsyn.2016.00006.

Branchereau P, Rodriguez JJ, Delvolvé I, Abrous DN, Le Moal M, Cabelguen JM. Serotonergic systems in the spinal cord of the amphibian urodele Pleurodeles waltl. *J Comp Neurol* 419: 49–60, 2000. doi:10.1002/(SICI)1096-9861(20000327)419:1<49:AID-CNE3>3.0.CO;2-#.

Brustein E, Chong M, Holmqvist B, Drapeau P. Serotonin patterns locomotor network activity in the developing zebrafish by modulating quiescent periods. *J Neurobiol* 57: 303–322, 2003. doi:10.1002/neu.10292.

Buchanan JT, Grillner S. 5-Hydroxytryptamine depresses reticulospinal excitatory postsynaptic potentials in motoneurons of the lamprey. *Neurosci Lett* 122: 71–74, 1991. doi:10.1016/0304-3940(91)90196-Z.

Cabelguen J-M, Bourcier-Lucas C, Dubuc R. Bimodal locomotion elicited by electrical stimulation of the midbrain in the salamander Notophthalmus viridescens. *J Neurosci* 23: 2434–2439, 2003. doi:10.1523/JNEUROSCI.23-06-02434.2003.

Cangiano L, Grillner S. Fast and slow locomotor burst generation in the hemispinal cord of the lamprey. *J Neurophysiol* 89: 2931–2942, 2003. doi:10.1152/jn.01100.2002.

Cangiano L, Grillner S. Mechanisms of rhythm generation in a spinal locomotor network deprived of crossed connections: the lamprey hemicord. *J Neurosci* 25: 923–935, 2005. doi:10.1523/JNEUROSCI.2301-04.2005.

Carrera I, Molist P, Anadón R, Rodríguez-Moldes I. Development of the serotoninergic system in the central nervous system of a shark, the lesser spotted dogfish Scyliorhinus canicula. *J Comp Neurol* 511: 804–831, 2008. doi:10.1002/cne.21857.

Cazalets JR, Sqalli-Houssaini Y, Clarac F. Activation of the central pattern generators for locomotion by serotonin and excitatory amino acids in neonatal rat. *J Physiol* 455: 187–204, 1992. doi:10.1113/jphysiol.1992.sp019296.

Cembrowski MS, Wang L, Lemire AL, Copeland M, DiLisio SF, Clements J, Spruston N. The subiculum is a patchwork of discrete subregions. *eLife* 7: e37701, 2018. doi:10.7554/eLife.37701.

Charrier V, Cabelguen J-M. Fictive rhythmic motor patterns produced by the tail spinal cord in salamanders. *Neuroscience* 255: 191–202, 2013. doi:10.1016/j.neuroscience.2013.10.020.

Cheng J, Jovanovic K, Aoyagi Y, Bennett DJ, Han Y, Stein RB. Differential distribution of interneurons in the neural networks that control walking in the mudpuppy (Necturus maculatus) spinal cord. *Exp Brain Res* 145: 190–198, 2002. doi:10.1007/s00221-002-1102-0.

Cheng J, Stein RB, Jovanović K, Yoshida K, Bennett DJ, Han Y. Identification, localization, and modulation of neural networks for walking in the mudpuppy (Necturus maculatus) spinal cord. *J Neurosci* 18: 4295–4304, 1998. doi:10.1523/JNEUROSCI.18-11-04295.1998.

Chevallier S, Landry M, Nagy F, Cabelguen J-M. Recovery of bimodal locomotion in the spinal-transected salamander, *Pleurodeles waltlii*. *Eur J Neurosci* 20: 1995–2007, 2004. doi:10.1111/j.1460-9568.2004.03671.x.

Chevallier S, Nagy F, Cabelguen J-M. Cholinergic control of excitability of spinal motoneurones in the salamander. *J Physiol* 570: 525–540, 2006. doi:10.1113/jphysiol.2005.098970.

Chevallier S, Nagy F, Cabelguen J-M. Muscarinic control of the excitability of hindlimb motoneurons in chronic spinal-transected salamanders. *Eur J Neurosci* 28: 2243–2253, 2008. doi:10.1111/j.1460-9568.2008.06506.x.

Chiba A. Serotonergic neuron system in the spinal cord of the gar Lepisosteus oculatus (Lepisosteiformes, Osteichthyes) with special regard to the juxtameningeal serotonergic plexus as a paracrine site. *Neurosci Lett* 413: 6–10, 2007. doi:10.1016/j.neulet.2006.10.068.

Chollet F, Tardy J, Albucher J-F, Thalamas C, Berard E, Lamy C, Bejot Y, Deltour S, Jaillard A, Niclot P, Guillon B, Moulin T, Marque P, Pariente J, Arnaud C, Loubinoux I. Fluoxetine for motor recovery after acute ischaemic stroke (FLAME): a randomised placebo-controlled trial. *Lancet Neurol* 10: 123–130, 2011. doi:10.1016/S1474-4422(10)70314-8.

Christenson J, Franck J, Grillner S. Increase in endogenous 5-hydroxytryptamine levels modulates the central network underlying locomotion in the lamprey spinal cord. *Neurosci Lett* 100: 188–192, 1989. doi:10.1016/0304-3940(89)90682-4.

Clairambault P, Christophe N, Pairault C, Herbin M, Ward R, Reperant J. Organization of the serotoninergic system in the brain of two amphibian species, *Ambystoma mexicanum* (Urodela) and *Typhlonectes compressicauda* (Gymnophiona). *Anat Embryol (Berl)* 190: 87–99, 1994. doi:10.1007/BF00185849.

Corio M, Thibault J, Peute J. Distribution of catecholaminergic and serotoninergic systems in forebrain and midbrain of the newt, Triturus alpestris (Urodela). *Cell Tissue Res* 268: 377–387, 1992. doi:10.1007/BF00318806.

Cotel F, Exley R, Cragg SJ, Perrier J-F. Serotonin spillover onto the axon initial segment of motoneurons induces central fatigue by inhibiting action potential initiation. *Proc Natl Acad Sci USA* 110: 4774–4779, 2013. doi:10.1073/pnas.1216150110.

Courtine G, Gerasimenko Y, van den Brand R, Yew A, Musienko P, Zhong H, Song B, Ao Y, Ichiyama RM, Lavrov I, Roy RR, Sofroniew MV, Edgerton VR. Transformation of nonfunctional spinal circuits into functional states after the loss of brain input. *Nat Neurosci* 12: 1333–1342, 2009. doi:10.1038/nn.2401.

Croul S, Radzievsky A, Sverstiuk A, Murray M. NK1, NMDA, 5HT1a, and 5HT2 receptor binding sites in the rat lumbar spinal cord: modulation following sciatic nerve crush. *Exp Neurol* 154: 66–79, 1998. doi:10.1006/exnr.1998.6875.

Daghfous G, Green WW, Alford ST, Zielinski BS, Dubuc R. Sensory activation of command cells for locomotion and modulatory mechanisms: lessons from lampreys. *Front Neural Circuits* 10: 18, 2016. doi:10.3389/fncir.2016.00018.

Dam M, Tonin P, De Boni A, Pizzolato G, Casson S, Ermani M, Freo U, Piron L, Battistin L. Effects of fluoxetine and maprotiline on functional recovery in poststroke hemiplegic patients undergoing rehabilitation therapy. *Stroke* 27: 1211–1214, 1996. doi:10.1161/01.STR.27.7.1211.

D'Amico JM, Butler AA, Héroux ME, Cotel F, Perrier JM, Butler JE, Gandevia SC, Taylor JL. Human motoneurone excitability is depressed by activation of serotonin 1A receptors with buspirone. *J Physiol* 595: 1763–1773, 2017. doi:10.1113/JP273200.

D'Amico JM, Murray KC, Li Y, Chan KM, Finlay MG, Bennett DJ, Gorassini MA. Constitutively active 5-HT2/α1 receptors facilitate muscle spasms after human spinal cord injury. *J Neurophysiol* 109: 1473–1484, 2013. doi:10.1152/jn.00821.2012.

Delay RJ, Kinnamon SC, Roper SD. Serotonin modulates voltage-dependent calcium current in Necturus taste cells. *J Neurophysiol* 77: 2515–2524, 1997. doi:10.1152/jn.1997.77.5.2515.

Delvolvé I, Branchereau P, Dubuc R, Cabelguen JM. Fictive rhythmic motor patterns induced by NMDA in an in vitro brain stem-spinal cord preparation from an adult urodele. *J Neurophysiol* 82: 1074–1077, 1999. doi:10.1152/jn.1999.82.2.1074.

Díaz-Ríos M, Dombeck DA, Webb WW, Harris-Warrick RM. Serotonin modulates dendritic calcium influx in commissural interneurons in the mouse spinal locomotor network. *J Neurophysiol* 98: 2157–2167, 2007. doi:10.1152/jn.00430.2007.

Dickstein DL, Dickstein DR, Janssen WGM, Hof PR, Glaser JR, Rodriguez A, O'Connor N, Angstman P, Tappan SJ. Automatic dendritic spine quantification from confocal data with neurolucida 360. *Curr Protoc Neurosci* 77: 1.27.1–1.27.21, 2016. doi:10.1002/cpns.16.

Dietz S, Husch A, Harris-Warrick RM. A comparison of serotonin neuromodulation of mouse spinal V2a interneurons using perforated patch and whole cell recording techniques. *Front Cell Neurosci* 6: 39, 2012. doi:10.3389/fncel.2012.00039.

Dimitrov D, Takagi H, Guillaud L, Saitoh N, Eguchi K, Takahashi T. Reconstitution of giant mammalian synapses in culture for molecular functional and imaging studies. *J Neurosci* 36: 3600–3610, 2016. doi:10.1523/JNEUROSCI.3869-15.2016.

Dubé L, Parent A. The organization of monoamine-containing neurons in the brain of the salamander, *Necturus maculosus. J Comp Neurol* 211: 21–30, 1982. doi:10.1002/cne.902110104.

Dunbar MJ, Tran MA, Whelan PJ. Endogenous extracellular serotonin modulates the spinal locomotor network of the neonatal mouse. *J Physiol* 588: 139–156, 2010. doi:10.1113/jphysiol.2009.177378.

Ericson J, Thor S, Edlund T, Jessell TM, Yamada T. Early stages of motor neuron differentiation revealed by expression of homeobox gene Islet-1. *Science* 256: 1555–1560, 1992. doi:10.1126/science.1350865.

Fabbiani G, Rehermann MI, Aldecosea C, Trujillo-Cenóz O, Russo RE. Emergence of serotonergic neurons after spinal cord injury in turtles. *Front Neural Circuits* 12: 20, 2018. doi:10.3389/fncir.2018.00020.

Fasolo A, Franzoni MF, Gaudino G, Steinbusch HW. The organization of serotonin-immunoreactive neuronal systems in the brain of the crested newt, *Triturus cristatus carnifex* Laur. *Cell Tissue Res* 243: 239–247, 1986. doi:10.1007/BF00251037.

Formento E, Minassian K, Wagner F, Mignardot JB, Le Goff-Mignardot CG, Rowald A, Bloch J, Micera S, Capogrosso M, Courtine G. Electrical spinal cord stimulation must preserve proprioception to enable locomotion in humans with spinal cord injury. *Nat Neurosci* 21: 1728–1741, 2018. doi:10.1038/s41593-018-0262-6.

Fouad K, Rank MM, Vavrek R, Murray KC, Sanelli L, Bennett DJ. Locomotion after spinal cord injury depends on constitutive activity in serotonin receptors. *J Neurophysiol* 104: 2975–2984, 2010. doi:10.1152/jn.00499.2010.

Francis ETB. *The Anatomy of the Salamander.* Oxford, UK: Clarendon, 1934.

Fredrich M, Reisch A, Illing R-B. Neuronal subtype identity in the rat auditory brainstem as defined by molecular profile and axonal projection. *Exp Brain Res* 195: 241–260, 2009. doi:10.1007/s00221-009-1776-7.

Gabriel JP, Mahmood R, Kyriakatos A, Söll I, Hauptmann G, Calabrese RL, El Manira A. Serotonergic modulation of locomotion in zebrafish: endogenous release and synaptic mechanisms. *J Neurosci* 29: 10387–10395, 2009. doi:10.1523/JNEUROSCI.1978-09.2009.

Gavin DP, Sharma RP, Chase KA, Matrisciano F, Dong E, Guidotti A. Growth arrest and DNA-damage-inducible, beta (GADD45b)-mediated DNA demethylation in major psychosis. *Neuropsychopharmacology* 37: 531–542, 2012. [Erratum in *Neuropsychopharmacology* 37: 2173, 2012]. doi:10.1038/npp.2011.221.

Gerachshenko T, Schwartz E, Bleckert A, Photowala H, Seymour A, Alford S. Presynaptic G-protein-coupled receptors dynamically modify vesicle fusion, synaptic cleft glutamate concentrations, and motor behavior. *J Neurosci* 29: 10221–10233, 2009. doi:10.1523/JNEUROSCI.1404-09.2009.

Gerasimenko YP, Ichiyama RM, Lavrov IA, Courtine G, Cai L, Zhong H, Roy RR, Edgerton VR. Epidural spinal cord stimulation plus quipazine administration enable stepping in complete spinal adult rats. *J Neurophysiol* 98: 2525–2536, 2007. doi:10.1152/jn.00836.2007.

Gourab K, Schmit BD, Hornby TG. Increased lower limb spasticity but not strength or function following a single-dose serotonin reuptake inhibitor in chronic stroke. *Arch Phys Med Rehabil* 96: 2112–2119, 2015. doi:10.1016/j.apmr.2015.08.431.

Gray MJ, Lewis JP, Nanjappa P, Klocke B, Pasmans F, Martel A, Stephen C, Parra Olea G, Smith SA, Sacerdote-Velat A, Christman MR, Williams JM, Olson DH. Batrachochytrium salamandrivorans: the North American response and a call for action. *PLoS Pathog* 11: e1005251, 2015. doi:10.1371/journal.ppat.1005251.

Grillner S. Control of locomotion in bipeds, tetrapods, and fish. In: *Handbook of Physiology. The Nervous System*, Motor Control, edited by Brookhart M. Bethesda, MD: American Physiological Society, 1981, p. 1179–1236. doi:10.1002/cphy.cp010226.

Hägglund M, Borgius L, Dougherty KJ, Kiehn O. Activation of groups of excitatory neurons in the mammalian spinal cord or hindbrain evokes locomotion. *Nat Neurosci* 13: 246–252, 2010. doi:10.1038/nn.2482.

Hägglund M, Dougherty KJ, Borgius L, Itohara S, Iwasato T, Kiehn O. Optogenetic dissection reveals multiple rhythmogenic modules underlying locomotion. *Proc Natl Acad Sci USA* 110: 11589–11594, 2013. doi:10.1073/pnas.1304365110.

Haraguchi S, Koyama T, Hasunuma I, Okuyama S, Ubuka T, Kikuyama S, Do Rego J-L, Vaudry H, Tsutsui K. Acute stress increases the synthesis of 7α-hydroxypregnenolone, a new key neurosteroid stimulating locomotor activity, through corticosterone action in newts. *Endocrinology* 153: 794–805, 2012. doi:10.1210/en.2011-1422.

Harris WA. Differences between embryos and adults in the plasticity of somatosensory afferents to the axolotl tectum. *Brain Res* 7: 245–255, 1983. doi:10.1016/0165-3806(83)90181-5.

Harris-Warrick RM, Cohen AH. Serotonin modulates the central pattern generator for locomotion in the isolated lamprey spinal cord. *J Exp Biol* 116: 27–46, 1985.

Harris-Warrick RM, McPhee JC, Filler JA. Distribution of serotonergic neurons and processes in the lamprey spinal cord. *Neuroscience* 14: 1127–1140, 1985. doi:10.1016/0306-4522(85)90282-9.

He H, Mahnke AH, Doyle S, Fan N, Wang C-C, Hall BJ, Tang Y-P, Inglis FM, Chen C, Erickson JD. Neurodevelopmental role for VGLUT2 in pyramidal neuron plasticity, dendritic refinement, and in spatial learning. *J Neurosci* 32: 15886–15901, 2012. doi:10.1523/JNEUROSCI.4505-11.2012.

Hubbard CS, Dolence EK, Rose JD. Brainstem reticulospinal neurons are targets for corticotropin-releasing factor-Induced locomotion in roughskin newts. *Horm Behav* 57: 237–246, 2010. doi:10.1016/j.yhbeh.2009.11.008.

Husch A, Dietz SB, Hong DN, Harris-Warrick RM. Adult spinal V2a interneurons show increased excitability and serotonin-dependent bistability. *J Neurophysiol* 113: 1124–1134, 2015. doi:10.1152/jn.00741.2014.

Husch A, Van Patten GN, Hong DN, Scaperotti MM, Cramer N, Harris-Warrick RM. Spinal cord injury induces serotonin supersensitivity without increasing intrinsic excitability of mouse V2a interneurons. *J Neurosci* 32: 13145–13154, 2012. doi:10.1523/JNEUROSCI.2995-12.2012.

Hutchinson SA, Eisen JS. Islet1 and Islet2 have equivalent abilities to promote motoneuron formation and to specify motoneuron subtype identity. *Development* 133: 2137–2147, 2006. doi:10.1242/dev.02355.

Jovanović K, Petrov T, Greer JJ, Stein RB. Serotonergic modulation of the mudpuppy (Necturus maculatus) locomotor pattern in vitro. *Exp Brain Res* 111: 57–67, 1996. doi:10.1007/BF00229556.

Jovanović K, Petrov T, Stein RB. Effects of inhibitory neurotransmitters on the mudpuppy (Necturus maculatus) locomotor pattern in vitro. *Exp Brain Res* 129: 172–184, 1999. doi:10.1007/s002210050887.

Kavanagh JJ, McFarland AJ, Taylor JL. Enhanced availability of serotonin increases activation of unfatigued muscle but exacerbates central fatigue during prolonged sustained contractions. *J Physiol* 597: 319–332, 2019. doi:10.1113/JP277148.

Kemp BJ, Krause JS. Depression and life satisfaction among people ageing with post-polio and spinal cord injury. *Disabil Rehabil* 21: 241–249, 1999. doi:10.1080/096382899297666.

Kiehn O. Decoding the organization of spinal circuits that control locomotion. *Nat Rev Neurosci* 17: 224–238, 2016. doi:10.1038/nrn.2016.9.

Knüsel J, Bicanski A, Ryczko D, Cabelguen J-M, Ijspeert AJ. A salamander's flexible spinal network for locomotion, modeled at two levels of abstraction. *Integr Comp Biol* 53: 269–282, 2013. doi:10.1093/icb/ict067.

Kornum BR, Licht CL, Weikop P, Knudsen GM, Aznar S. Central serotonin depletion affects rat brain areas differently: a qualitative and quantitative comparison between different treatment schemes. *Neurosci Lett* 392: 129–134, 2006. doi:10.1016/j.neulet.2005.09.013.

Lamotte CC, Johns DR, de Lanerolle NC. Immunohistochemical evidence of indolamine neurons in monkey spinal cord. *J Comp Neurol* 206: 359–370, 1982. doi:10.1002/cne.902060404.

Landry ES, Lapointe NP, Rouillard C, Levesque D, Hedlund PB, Guertin PA. Contribution of spinal 5-HT1A and 5-HT7 receptors to locomotor-like movement induced by 8-OH-DPAT in spinal cord-transected mice. *Eur J Neurosci* 24: 535–546, 2006. doi:10.1111/j.1460-9568.2006.04917.x.

Lavrov I, Cheng J. Methodological optimization of applying neuroactive agents for the study of locomotor-like activity in the mudpuppies (Necturus maculatus). *J Neurosci Methods* 174: 97–102, 2008. doi:10.1016/j.jneumeth.2008.07.010.

Le Ray D, Brocard F, Bourcier-Lucas C, Auclair F, Lafaille P, Dubuc R. Nicotinic activation of reticulospinal cells involved in the control of swimming in lampreys. *Eur J Neurosci* 17: 137–148, 2003. doi:10.1046/j.1460-9568.2003.02417.x.

Leech KA, Kinnaird CR, Hornby TG. Effects of serotonergic medications on locomotor performance in humans with incomplete spinal cord injury. *J Neurotrauma* 31: 1334–1342, 2014. doi:10.1089/neu.2013.3206.

Liang C-L, Quang Nguyen T, Marks GA. Inhibitory and excitatory amino acid neurotransmitters are utilized by the projection from the dorsal deep mesencephalic nucleus to the sublaterodorsal nucleus REM sleep induction zone. *Brain Res* 1567: 1–12, 2014. doi:10.1016/j.brainres.2014.04.016.

Lillesaar C, Tannhäuser B, Stigloher C, Kremmer E, Bally-Cuif L. The serotonergic phenotype is acquired by converging genetic mechanisms within the zebrafish central nervous system. *Dev Dyn* 236: 1072–1084, 2007. doi:10.1002/dvdy.21095.

Lin LH, Emson PC, Talman WT. Apposition of neuronal elements containing nitric oxide synthase and glutamate in the nucleus tractus solitarii of rat: a confocal microscopic analysis. *Neuroscience* 96: 341–350, 2000. doi:10.1016/S0306-4522(99)00560-6.

Liu J, Hunter CS, Du A, Ediger B, Walp E, Murray J, Stein R, May CL. Islet-1 regulates Arx transcription during pancreatic islet alpha-cell development. *J Biol Chem* 286: 15352–15360, 2011. doi:10.1074/jbc.M111.231670.

Lowry CA, Burke KA, Renner KJ, Moore FL, Orchinik M. Rapid changes in monoamine levels following administration of corticotropin-releasing factor or corticosterone are localized in the dorsomedial hypothalamus. *Horm Behav* 39: 195–205, 2001. doi:10.1006/hbeh.2001.1646.

Lowry CA, Hale MW, Burke KA, Renner KJ, Moore FL. Fluoxetine potentiates the effects of corticotropin-releasing factor on locomotor activity and serotonergic systems in the roughskin newt, *Taricha granulosa*. *Horm Behav* 56: 177–184, 2009. doi:10.1016/j.yhbeh.2009.04.006.

Lowry CA, Renner KJ, Moore FL. Catecholamines and indoleamines in the central nervous system of a urodele amphibian: a microdissection study with emphasis on the distribution of epinephrine. *Brain Behav Evol* 48: 70–93, 1996. doi:10.1159/000113187.

Madriaga MA, McPhee LC, Chersa T, Christie KJ, Whelan PJ. Modulation of locomotor activity by multiple 5-HT and dopaminergic receptor subtypes in the neonatal mouse spinal cord. *J Neurophysiol* 92: 1566–1576, 2004. doi:10.1152/jn.01181.2003.

Marder E, O'Leary T, Shruti S. Neuromodulation of circuits with variable parameters: single neurons and small circuits reveal principles of state-

dependent and robust neuromodulation. *Annu Rev Neurosci* 37: 329–346, 2014. doi:10.1146/annurev-neuro-071013-013958.

Marín O, Smeets WJ, González A. Distribution of choline acetyltransferase immunoreactivity in the brain of anuran (*Rana perezi, Xenopus laevis*) and urodele (*Pleurodeles waltl*) amphibians. *J Comp Neurol* 382: 499–534, 1997. doi:10.1002/(SICI)1096-9861(19970616)382:4<499:AID-CNE6>3.0.CO;2-Y.

Massouh M, Wallman M-J, Pourcher E, Parent A. The fate of the large striatal interneurons expressing calretinin in Huntington's disease. *Neurosci Res* 62: 216–224, 2008. doi:10.1016/j.neures.2008.08.007.

Matsushima T, Grillner S. Local serotonergic modulation of calcium-dependent potassium channels controls intersegmental coordination in the lamprey spinal cord. *J Neurophysiol* 67: 1683–1690, 1992. doi:10.1152/jn.1992.67.6.1683.

McLean DL, Fetcho JR. Ontogeny and innervation patterns of dopaminergic, noradrenergic, and serotonergic neurons in larval zebrafish. *J Comp Neurol* 480: 38–56, 2004. doi:10.1002/cne.20280.

McLean DL, Sillar KT. Divergent actions of serotonin receptor activation during fictive swimming in frog embryos. *J Comp Physiol A Neuroethol Sens Neural Behav Physiol* 190: 391–402, 2004. doi:10.1007/s00359-004-0504-9.

Meuser T, Pietruck C, Gabriel A, Xie G-X, Lim K-J, Pierce Palmer P. 5-HT7 receptors are involved in mediating 5-HT-induced activation of rat primary afferent neurons. *Life Sci* 71: 2279–2289, 2002. doi:10.1016/S0024-3205(02)02011-8.

Montgomery JE, Wahlstrom-Helgren S, Wiggin TD, Corwin BM, Lillesaar C, Masino MA. Intraspinal serotonergic signaling suppresses locomotor activity in larval zebrafish. *Dev Neurobiol* 78: 807–827, 2018. doi:10.1002/dneu.22606.

Montgomery JE, Wiggin TD, Rivera-Perez LM, Lillesaar C, Masino MA. Intraspinal serotonergic neurons consist of two, temporally distinct populations in developing zebrafish. *Dev Neurobiol* 76: 673–687, 2016. doi:10.1002/dneu.22352.

Mor Y, Lev-Tov A. Analysis of rhythmic patterns produced by spinal neural networks. *J Neurophysiol* 98: 2807–2817, 2007. doi:10.1152/jn.00740.2007.

Moreno N, González A. Regionalization of the telencephalon in urodele amphibians and its bearing on the identification of the amygdaloid complex. *Front Neuroanat* 1: 1, 2007. doi:10.3389/neuro.05.001.2007.

Moreno N, López JM, Morona R, Lozano D, Jiménez S, González A. Comparative analysis of Nkx2.1 and Islet-1 expression in urodele amphibians and lungfishes highlights the pattern of forebrain organization in early tetrapods. *Front Neuroanat* 12: 42, 2018. doi:10.3389/fnana.2018.00042.

Musienko P, van den Brand R, Märzendorfer O, Roy RR, Gerasimenko Y, Edgerton VR, Courtine G. Controlling specific locomotor behaviors through multidimensional monoaminergic modulation of spinal circuitries. *J Neurosci* 31: 9264–9278, 2011. doi:10.1523/JNEUROSCI.5796-10.2011.

Newton BW, Maley BE, Hamill RW. Immunohistochemical demonstration of serotonin neurons in autonomic regions of the rat spinal cord. *Brain Res* 376: 155–163, 1986. doi:10.1016/0006-8993(86)90910-8.

Norris DO, Carr JA, Desan PH, Smock TK, Norman MF. Monoamines and their metabolites in the amphibian (*Ambystoma tigrinum*) brain: quantitative changes during metamorphosis and captivity. *Comp Biochem Physiol Part A Physiol* 103: 279–283, 1992. doi:10.1016/0300-9629(92)90580-J.

O'Brien KB, Esguerra M, Miller RF, Bowser MT. Monitoring neurotransmitter release from isolated retinas using online microdialysis-capillary electrophoresis. *Anal Chem* 76: 5069–5074, 2004. doi:10.1021/ac049822v.

Ohnmacht J, Yang Y, Maurer GW, Barreiro-Iglesias A, Tsarouchas TM, Wehner D, Sieger D, Becker CG, Becker T. Spinal motor neurons are regenerated after mechanical lesion and genetic ablation in larval zebrafish. *Development* 143: 1464–1474, 2016. doi:10.1242/dev.129155.

Otoshi CK, Walwyn WM, Tillakaratne NJK, Zhong H, Roy RR, Edgerton VR. Distribution and localization of 5-HT(1A) receptors in the rat lumbar spinal cord after transection and deafferentation. *J Neurotrauma* 26: 575–584, 2009. doi:10.1089/neu.2008.0640.

Oueghlani Z, Juvin L, Lambert FM, Cardoit L, Courtand G, Masmejean F, Cazalets J-R, Barrière G. Serotonergic modulation of sacral dorsal root stimulation-induced locomotor output in newborn rat. *Neuropharmacology* 170: 107815, 2020. doi:10.1016/j.neuropharm.2019.107815.

Parent A, Northcutt RG. The monoamine-containing neurons in the brain of the garfish, *Lepisosteus osseus*. *Brain Res Bull* 9: 189–204, 1982. doi:10.1016/0361-9230(82)90132-0.

Pearlstein E, Ben Mabrouk F, Pflieger JF, Vinay L. Serotonin refines the locomotor-related alternations in the in vitro neonatal rat spinal cord. *Eur J Neurosci* 21: 1338–1346, 2005. doi:10.1111/j.1460-9568.2005.03971.x.

Pedroni A, Ampatzis K. Large-scale analysis of the diversity and complexity of the adult spinal cord neurotransmitter typology. *iScience* 19: 1189–1201, 2019. doi:10.1016/j.isci.2019.09.010.

Perrier J-F. If serotonin does not exhaust you, it makes you stronger. *J Physiol* 597: 5–6, 2019. doi:10.1113/JP277317.

Perrier J-F, Cotel F. Serotonin differentially modulates the intrinsic properties of spinal motoneurons from the adult turtle. *J Physiol* 586: 1233–1238, 2008. doi:10.1113/jphysiol.2007.145706.

Perrier J-F, Cotel F. Serotonergic modulation of spinal motor control. *Curr Opin Neurobiol* 33: 1–7, 2015. doi:10.1016/j.conb.2014.12.008.

Perrier J-F, Delgado-Lezama R. Synaptic release of serotonin induced by stimulation of the raphe nucleus promotes plateau potentials in spinal motoneurons of the adult turtle. *J Neurosci* 25: 7993–7999, 2005. doi:10.1523/JNEUROSCI.1957-05.2005.

Perrier J-F, Rasmussen HB, Jørgensen LK, Berg RW. Intense activity of the raphe spinal pathway depresses motor activity via a serotonin dependent mechanism. *Front Neural Circuits* 11: 111, 2018. doi:10.3389/fncir.2017.00111.

Perrin FE, Gerber YN, Teigell M, Lonjon N, Boniface G, Bauchet L, Rodriguez JJ, Hugnot JP, Privat AM. Anatomical study of serotonergic innervation and 5-HT(1A) receptor in the human spinal cord. *Cell Death Dis* 2: e218, 2011. doi:10.1038/cddis.2011.98.

Photowala H, Blackmer T, Schwartz E, Hamm HE, Alford S. G protein βγ-subunits activated by serotonin mediate presynaptic inhibition by regulating vesicle fusion properties. *Proc Natl Acad Sci USA* 103: 4281–4286, 2006. doi:10.1073/pnas.0600509103.

Pombal MA, Marín O, González A. Distribution of choline acetyltransferase-immunoreactive structures in the lamprey brain. *J Comp Neurol* 431: 105–126, 2001. doi:10.1002/1096-9861(20010226)431:1<105:AID-CNE1058>3.0.CO;2-P.

Quinlan KA, Buchanan JT. Cellular and synaptic actions of acetylcholine in the lamprey spinal cord. *J Neurophysiol* 100: 1020–1031, 2008. doi:10.1152/jn.01157.2007.

Reimer MM, Sörensen I, Kuscha V, Frank RE, Liu C, Becker CG, Becker T. Motor neuron regeneration in adult zebrafish. *J Neurosci* 28: 8510–8516, 2008. doi:10.1523/JNEUROSCI.1189-08.2008.

Reyes-Ruiz JM, Limon A, Korn MJ, Nakamura PA, Shirkey NJ, Wong JK, Miledi R. Profiling neurotransmitter receptor expression in the *Ambystoma mexicanum* brain. *Neurosci Lett* 538: 32–37, 2013. doi:10.1016/j.neulet.2013.01.015.

Ribas-Salgueiro JL, Gaytán SP, Ribas J, Pásaro R. Characterization of efferent projections of chemosensitive neurons in the caudal parapyramidal area of the rat brain. *Brain Res Bull* 66: 235–248, 2005. doi:10.1016/j.brainresbull.2005.05.014.

Ritchie TC, Leonard RB. Immunocytochemical demonstration of serotonergic cells, terminals and axons in the spinal cord of the stingray, Dasyatis sabina. *Brain Res* 240: 334–337, 1982. doi:10.1016/0006-8993(82)90230-X.

Ritchie TC, Roos LJ, Williams BJ, Leonard RB. The descending and intrinsic serotoninergic innervation of an elasmobranch spinal cord. *J Comp Neurol* 224: 395–406, 1984. doi:10.1002/cne.902240307.

Rodriguez A, Ehlenberger DB, Hof PR, Wearne SL. Three-dimensional neuron tracing by voxel scooping. *J Neurosci Methods* 184: 169–175, 2009. doi:10.1016/j.jneumeth.2009.07.021.

Rossignol S, Frigon A. Recovery of locomotion after spinal cord injury: some facts and mechanisms. *Annu Rev Neurosci* 34: 413–440, 2011. doi:10.1146/annurev-neuro-061010-113746.

Ryczko D, Auclair F, Cabelguen J-M, Dubuc R. The mesencephalic locomotor region sends a bilateral glutamatergic drive to hindbrain reticulospinal neurons in a tetrapod. *J Comp Neurol* 524: 1361–1383, 2016a. doi:10.1002/cne.23911.

Ryczko D, Charrier V, Ijspeert A, Cabelguen J-M. Segmental oscillators in axial motor circuits of the salamander: distribution and bursting mechanisms. *J Neurophysiol* 104: 2677–2692, 2010. doi:10.1152/jn.00479.2010.

Ryczko D, Cone JJ, Alpert MH, Goetz L, Auclair F, Dubé C, Parent M, Roitman MF, Alford S, Dubuc R. A descending dopamine pathway conserved from basal vertebrates to mammals. *Proc Natl Acad Sci USA* 113: E2440–E2449, 2016b. doi:10.1073/pnas.1600684113.

Ryczko D, Grätsch S, Auclair F, Dubé C, Bergeron S, Alpert MH, Cone JJ, Roitman MF, Alford S, Dubuc R. Forebrain dopamine neurons project down to a brainstem region controlling locomotion. *Proc Natl Acad Sci USA* 110: E3235–E3242, 2013. doi:10.1073/pnas.1301125110.

Ryczko D, Grätsch S, Schläger L, Keuyalian A, Boukhatem Z, Garcia C, Auclair F, Büschges A, Dubuc R. Nigral glutamatergic neurons control the speed of locomotion. *J Neurosci* 37: 9759–9770, 2017. doi:10.1523/JNEUROSCI.1810-17.2017.

Ryczko D, Knüsel J, Crespi A, Lamarque S, Mathou A, Ijspeert AJ, Cabelguen JM. Flexibility of the axial central pattern generator network for locomotion in the salamander. *J Neurophysiol* 113: 1921–1940, 2015. doi:10.1152/jn.00894.2014.

Sako H, Kojima T, Okado N. Immunohistochemical study on the development of serotoninergic neurons in the chick: II. Distribution of cell bodies and fibers in the spinal cord. *J Comp Neurol* 253: 79–91, 1986. doi:10.1002/cne.902530107.

Schotland JL, Shupliakov O, Grillner S, Brodin L. Synaptic and nonsynaptic monoaminergic neuron systems in the lamprey spinal cord. *J Comp Neurol* 372: 229–244, 1996. doi:10.1002/(SICI)1096-9861(19960819)372:2<229:AID-CNE6>3.0.CO;2-5.

Sharples SA, Whelan PJ. Modulation of rhythmic activity in mammalian spinal networks is dependent on excitability state. *eNeuro* 4: ENEURO.0368–16.2017, 2017.

Sholl DA. Dendritic organization in the neurons of the visual and motor cortices of the cat. *J Anat* 87: 387–406, 1953.

Sims TJ. The development of monamine-containing neurons in the brain and spinal cord of the salamander, Ambystoma mexicanum. *J Comp Neurol* 173: 319–335, 1977. doi:10.1002/cne.901730208.

Sławińska U, Miazga K, Jordan LM. 5-HT$_2$ and 5-HT$_7$ receptor agonists facilitate plantar stepping in chronic spinal rats through actions on different populations of spinal neurons. *Front Neural Circuits* 8: 95, 2014a. doi:10.3389/fncir.2014.00095.

Sławińska U, Miazga K, Jordan LM. The role of serotonin in the control of locomotor movements and strategies for restoring locomotion after spinal cord injury. *Acta Neurobiol Exp (Wars)* 74: 172–187, 2014b.

Sqalli-Houssaini Y, Cazalets JR, Clarac F. Oscillatory properties of the central pattern generator for locomotion in neonatal rats. *J Neurophysiol* 70: 803–813, 1993. doi:10.1152/jn.1993.70.2.803.

Takahashi M, Freed R, Blackmer T, Alford S. Calcium influx-independent depression of transmitter release by 5-HT at lamprey spinal cord synapses. *J Physiol* 532: 323–336, 2001. doi:10.1111/j.1469-7793.2001.0323f.x.

Takeoka A, Vollenweider I, Courtine G, Arber S. Muscle spindle feedback directs locomotor recovery and circuit reorganization after spinal cord injury. *Cell* 159: 1626–1639, 2014. doi:10.1016/j.cell.2014.11.019.

Tang Y, Peng Z, Tao S, Sun J, Wang W, Guo X, Liu G, Luo X, Chen Y, Shen Y, Ma H, Xu P, Li Q, Zhang H, Feng Z. VGLUT2/Cdk5/p25 signaling pathway contributed to inflammatory pain by complete Freund's adjuvant. *Pain Res Manag* 2020: 4807674, 2020. doi:10.1155/2020/4807674.

Terada N, Ohno N, Saitoh S, Saitoh Y, Ohno S. Immunoreactivity of glutamate in mouse retina inner segment of photoreceptors with in vivo cryotechnique. *J Histochem Cytochem* 57: 883–888, 2009. doi:10.1369/jhc.2009.953851.

Thompson CK, Hornby TG. Divergent modulation of clinical measures of volitional and reflexive motor behaviors following serotonergic medications in human incomplete spinal cord injury. *J Neurotrauma* 30: 498–502, 2013. doi:10.1089/neu.2012.2515.

Thor KB, Nickolaus S, Helke CJ. Autoradiographic localization of 5-hydroxytryptamine1A, 5-hydroxytryptamine1B and 5-hydroxytryptamine1C/2 binding sites in the rat spinal cord. *Neuroscience* 55: 235–252, 1993. doi:10.1016/0306-4522(93)90469-V.

Tsuchida T, Ensini M, Morton SB, Baldassare M, Edlund T, Jessell TM, Pfaff SL. Topographic organization of embryonic motor neurons defined by expression of LIM homeobox genes. *Cell* 79: 957–970, 1994. doi:10.1016/0092-8674(94)90027-2.

van den Brand R, Heutschi J, Barraud Q, DiGiovanna J, Bartholdi K, Huerlimann M, Friedli L, Vollenweider I, Moraud EM, Duis S, Dominici N, Micera S, Musienko P, Courtine G. Restoring voluntary control of locomotion after paralyzing spinal cord injury. *Science* 336: 1182–1185, 2012. doi:10.1126/science.1217416.

Van Dongen PA, Hökfelt T, Grillner S, Verhofstad AA, Sternbusch HW, Cuello AC, Terenius L. Immunohistochemical demonstration of some putative neurotransmitters in the lamprey spinal cord and spinal ganglia: 5-hydroxytryptamine-, tachykinin-, and neuropeptide-Y-immunoreactive neurons and fibers. *J Comp Neurol* 234: 501–522, 1985. doi:10.1002/cne.902340408.

Verma P, Augustine GJ, Ammar M-R, Tashiro A, Cohen SM. A neuroprotective role for microRNA miR-1000 mediated by limiting glutamate excitotoxicity. *Nat Neurosci* 18: 379–385, 2015. doi:10.1038/nn.3935.

Wang SY, Liu X, Yianni J, Christopher Miall R, Aziz TZ, Stein JF. Optimising coherence estimation to assess the functional correlation of tremor-related activity between the subthalamic nucleus and the forearm muscles. *J Neurosci Methods* 136: 197–205, 2004. doi:10.1016/j.jneumeth.2004.01.008.

Wang D, Grillner S, Wallén P. 5-HT and dopamine modulates CaV1.3 calcium channels involved in postinhibitory rebound in the spinal network for locomotion in lamprey. *J Neurophysiol* 105: 1212–1224, 2011. doi:10.1152/jn.00324.2009.

Wang L, Ennis M, Szabó G, Armstrong WE. Characteristics of GABAergic and cholinergic neurons in perinuclear zone of mouse supraoptic nucleus. *J Neurophysiol* 113: 754–767, 2015. doi:10.1152/jn.00561.2014.

Wikström M, Hill R, Hellgren J, Grillner S. The action of 5-HT on calcium-dependent potassium channels and on the spinal locomotor network in lamprey is mediated by 5-HT1A-like receptors. *Brain Res* 678: 191–199, 1995. doi:10.1016/0006-8993(95)00183-Q.

Woodrow L, Sheppard P, Gardiner PF. Transcriptional changes in rat α-motoneurons resulting from increased physical activity. *Neuroscience* 255: 45–54, 2013. doi:10.1016/j.neuroscience.2013.09.038.

Xiao X, Djurisic M, Hoogi A, Sapp RW, Shatz CJ, Rubin DL. Automated dendritic spine detection using convolutional neural networks on maximum intensity projected microscopic volumes. *J Neurosci Methods* 309: 25–34, 2018. doi:10.1016/j.jneumeth.2018.08.019.

Xu P, Cao X, He Y, Zhu L, Yang Y, Saito K, Wang C, Yan X, Hinton AO Jr, Zou F, Ding H, Xia Y, Yan C, Shu G, Wu S-P, Yang B, Feng Y, Clegg DJ, DeMarchi R, Khan SA, Tsai SY, DeMayo FJ, Wu Q, Tong Q, Xu Y. Estrogen receptor-α in medial amygdala neurons regulates body weight. *J Clin Invest* 125: 2861–2876, 2015. doi:10.1172/JCI80941.

Yamamoto Y, Henderson CE. Patterns of programmed cell death in populations of developing spinal motoneurons in chicken, mouse, and rat. *Dev Biol* 214: 60–71, 1999. doi:10.1006/dbio.1999.9413.

Yokogawa T, Hannan MC, Burgess HA. The dorsal raphe modulates sensory responsiveness during arousal in zebrafish. *J Neurosci* 32: 15205–15215, 2012. doi:10.1523/JNEUROSCI.1019-12.2012.

Zhang W, Pombal MA, el Manira A, Grillner S. Rostrocaudal distribution of 5-HT innervation in the lamprey spinal cord and differential effects of 5-HT on fictive locomotion. *J Comp Neurol* 374: 278–290, 1996. doi:10.1002/(SICI)1096-9861(19961014)374:2<278:AID-CNE9>3.0.CO;2-#.

Zhong G, Droho S, Crone SA, Dietz S, Kwan AC, Webb WW, Sharma K, Harris-Warrick RM. Electrophysiological characterization of V2a interneurons and their locomotor-related activity in the neonatal mouse spinal cord. *J Neurosci* 30: 170–182, 2010. doi:10.1523/JNEUROSCI.4849-09.2010.